UNIVERSITY OF THESSALY

SCHOOL OF HEALTH SCIENCES

DEPARTMENT OF BIOCHEMISTRY-BIOTECHNOLOGY

Msc in Toxicology

HISTOPATHOLOGICAL EVALUATION, APOPTOSIS AND REDOX ASSESSMENT IN KIDNEY TISSUES IN A CONTRAST- INDUCED RABBIT NEPHROTOXICITY MODEL

MASTER THESIS

Maria- Malvina Tsamouri, DVM, Msc Candidate

Larissa, 2017

HISTOPATHOLOGICAL EVALUATION, APOPTOSIS AND REDOX ASSESSMENT IN KIDNEY TISSUES IN A CONTRAST- INDUCED RABBIT NEPHROTOXICITY MODEL

Advisory Committee:

- Dr. Aristides Tsatsakis : Chemist, PhD, ERT, Toxicology Science and Research Centre, Department of Forensic Sciences, Medical School, University of Crete
- Dr. Charitini Nepka : MD, PhD, Cytopathologist, Pathology Department, University Hospital of Larissa
- Dr. ChristinaTsitsimpikou Chemist, Msc, PhD, ERT, General Chemical State Laboratory of Greece

ACKNOWLEDGMENTS

This thesis was a challenge for me. The opportunity was given to combine my Veterinary degree with the new knowledge and skills I acquired in the field of Toxicology.

I would like to thank my family, especially my *parents* and *grandparents* for their moral and financial support throughout my studies. They have always been there for me and I am thankful for everything they have helped me achieve. In addition, I should thank my *dearest friends* for their love and support.

I would like to thank Professor *Aristides Tsatsakis*, Dr *Christina Tsitsimpikou* and Professor *Dimitris Kouretas* for their scientific contribution to this project. Special thanks should be attributed to PhD student *Paraskevi Kouka* for her valuable assistance.

Finally, this thesis could not have been realized without the guidance, mentoring and support of my teacher, Dr. *Charitini Nepka*. It was really pleasant to work with her, our collaboration was outstanding and lead to this great result.

Chalkida, 15/12/2016,

Maria- Malvina Tsamouri,

Doctor of Veterinary Medicine, Msc in Toxicology Candidate

CONTENTS

TABLES

FIGURES

ABSTRACT

Introduction: With the increasing use of iodinated contrast-media (CM) in diagnostic and interventional procedures, contrast-induced nephropathy (CIN) has become the third leading cause of hospital- acquired acute kidney injury. The pathophysiology of this condition remains unclear and is probably related to a combination of hemodynamic alterations, direct renal tubular cell toxicity and reactive oxygen species (ROS) production. However, existing animal models are not fully comparable to humans, as prior exposure to multiple renal insults is needed to induce CIN in animals with normal renal function.

Materials & Methods: In an attempt to shed more light to this condition, 9 male new Zealand White rabbits were randomized and divided into three groups(n=3 each): i) control group, ii) 24hCIN group and iii) 48hCIN group. The CIN model involved intravenous administration of the non- ionic, low- osmolar iodinated contrast media iopromide, 8g/kg body weight. Blood collection was performed at 2h, 10h, 24h and 48h for urea and creatinine measurements. Control and 48hCIN groups were euthanized at 48 hours whereas 24hCIN group at 24hours. Oxidative stress biomarkers, namely total antioxidant capacity (TAC), catalase (CAT), protein carbonyls (PC), and lipid peroxidation (TBARS) were evaluated in three anatomical renal areas (medulla, cortex, juxtamedullary) at 24 and 48 hours. Histopathological evaluation of the kidneys was also performed with four different special stains as well as assessment of apoptosis.

Results: Creatinine measurements indicated CIN existence. In kidney tissues, no statistically significant differences were observed in oxidation reduction markers, except for a reduction of CAT in renal cortex between control and 48hCIN groups (39, 6%). Extended tubular vacuolization in cortical and juxtamedullary zone were also present that was statistically correlated with urea and creatinine levels. TUNEL assay did not depict any apoptotic phenomena.

Discussion: The rabbit nephrotoxicity model was successful. Biochemical parameters showed that mechanisms exist that counterbalanced renal insult around 24 hours followed by the peak of ROS production. Apoptosis did not occur. Future research on our model may unlock more aspects of the condition.

1. Introduction of contrast induced nephropathy (CIN)

Recent advances in medical technology have led to an increased use of iodinated contrast media in diagnostic, radiographic and interventional procedures (Seeliger et al, 2012). Despite the advances in molecular structures, all contrast media may show adverse effects, ranging from mild to severe, and most importantly, they can show severe toxicity on renal tubular cells, resulting in a condition known as contrast induced nephropathy(CIN) (Mc Cullough PA, 2008) .CIN is defined by the European Society of Urogenital Radiology as "an increase in serum creatinine (SC) of at least 25% or 44 μmol/l within 3 days after the intravascular administration of an iodinated contrast medium (CM) in the absence of an alternative aetiology" (Stacul et al, 2011). CIN is the third leading cause of hospital-acquired acute renal failure (Asif, Epstein, 2004).

Although most cases of CIN involve mild and transient impairment of renal function, it may be permanent even, in some cases, resulting in chronic renal failure, with the need for permanent dialysis (Gruberg, 2001). The development of CIN is associated with marked morbidity and mortality, as well as longer hospital admissions (Subramanian et al, 2007) with increased costs of medical care, end stage renal disease (Majumdar, 2009), need for dialysis (Guastoni et al, 2014), and increased short and long term mortality (Mc Cullough PA, 2008). Annually, approximately, 150000 patients experience CIN and at least 1% require dialysis and prolonged hospital stay. Dialysis is calculated to cost approximately $32 million each year and the mean 2- day increase in length of stay can add $148 million (Barreto, 2007). With the rapid increase in the number of procedures that involve the use of contrast media, more light should be shed to the pathophysiology and mechanisms of contrast media- induced- acute kidney injury, so that the referring physicians would better understand the short- and long-term consequences in patients who develop CIN.

1.1 Functional Anatomy

In order to understand the underlying mechanisms of CIN a review of the renal anatomy and vasculature is essential. The functional unit of the kidney is the nephron, which is further divided in the glomerulus, proximal convoluted tubules, descending and ascending limbs of the loops of Henle, distal convoluted tubules, juxtaglomerular apparatus, connecting segment, collecting ducts and interstitium (Figure 1).

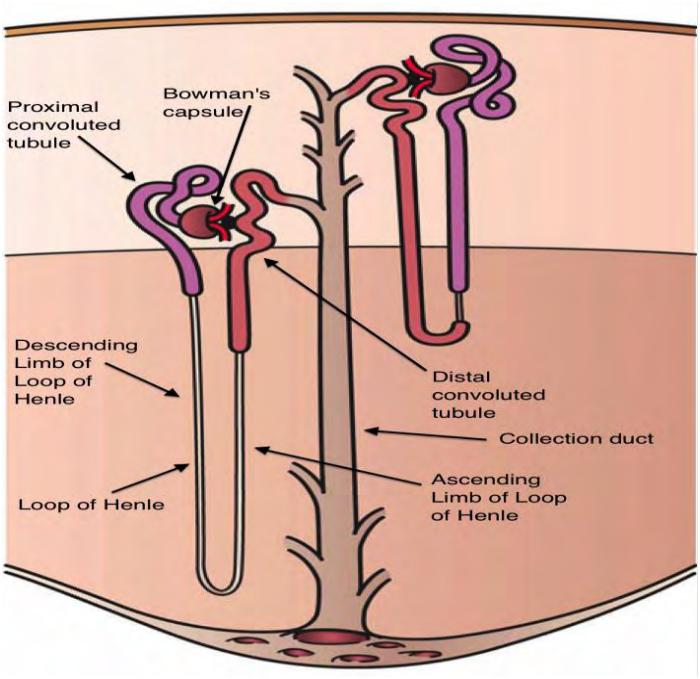

Figure 1: Nephron: the functional unit of the kidney

The kidney can also be divided into five topographic zones: cortex, outer and inner stripe of the outer medulla, inner medulla and papilla (Figure 2).

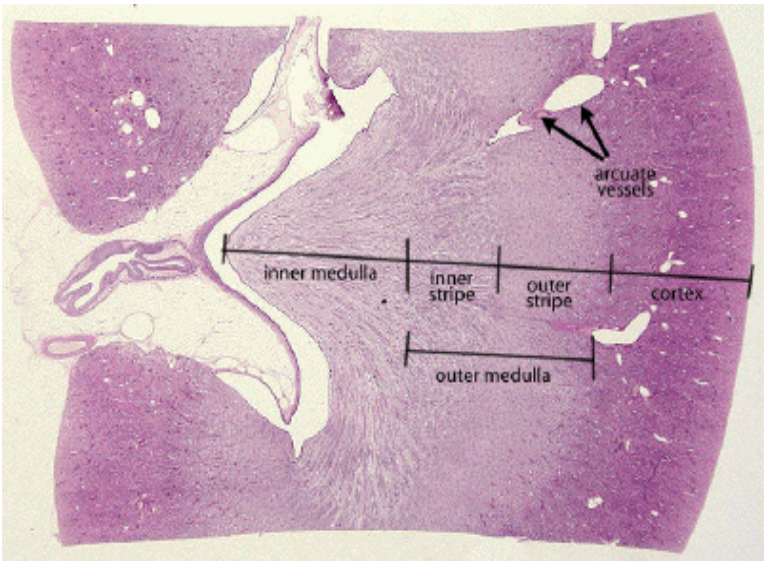

Figure 2: Basic kidney topographic zones of a rabbit

As far as the renal vascular supply is concerned, blood from the systemic circulation travels to the kidney via the renal artery, enters interlobar arteries and then arcuate arteries that run parallel to the capsule along the corticomedullary junction. They continue as interlobular arteries, afferent arterioles that delivers blood to the glomerular

capillaries of the nephron. Then, the efferent arterioles that arise from the glomeruli near the medulla, give rise to interconnecting vasa recta that offer blood supply to the medulla (Figure 3). These vessels is then analyzed (reversely in comparison to the arteries) in a capillary network that leads to vein formation and finally, the renal vein that exerts the kidney (Sahota et al, 2013). Renal blood flow is unique, as afferent and efferent arterioles control blood flow through renal capillaries (Mihail, 2010).

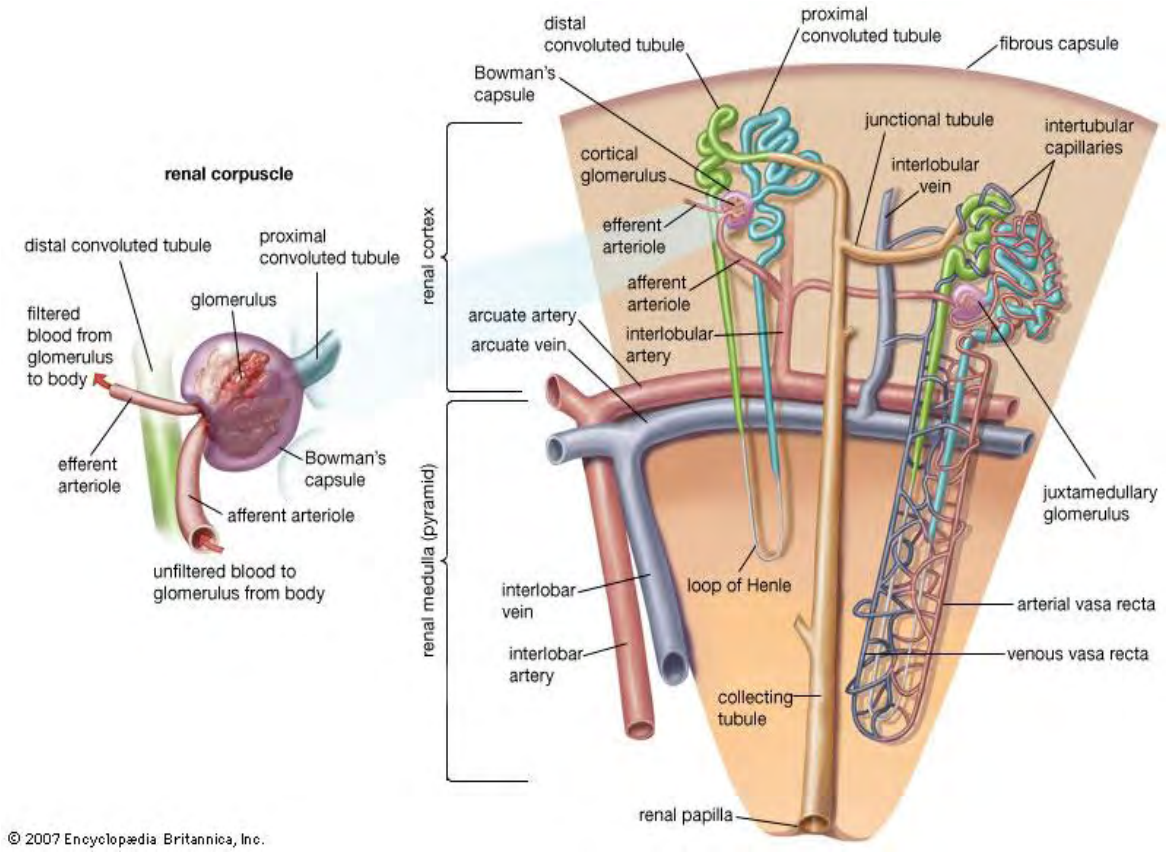

Figure 3: Detailed image of renal vasculature

1.2 Types of contrast media

Contrast media that are used for X-ray procedures, are tri-iodinated benzene derivatives that show radio-opacity due to iodine (Sendeski, 2011). The higher iodine concentration, and subsequently the molar concentration of benzene derivatives, the higher attenuation is achieved. Molar concentration defines two very important physicochemical properties that are implicated to CIN: osmolality and viscosity.

The necessity to produce contrast- media that would offer high attenuation with the minimum side effects, led to a diverse family of compounds, each with different effects and physicochemical properties (Tumlin et al, 2006). As far as osmolarity is concerned, there are four types of iodinated contrast media:

- *high-osmolar ionic monomers* (osmolarities 1000–2500 mosmol/kg H_2O),
- *low-osmolar ionic dimers* (osmolarity: 400–800 mosmol/kg H_2O),
- *low-osmolar non-ionic monomers* (osmolarity: 400-800 mosmol/kg H_2O) and
- *iso-osmolar non-ionic dimers* (osmolarity: 290 mosmol/kg H_20)(Geenen et al, 2013).

It should be noted that the osmolarity of low-osmolar contrast media is higher than that of the plasma (290 mosmol/kg H_2O) (Pannu et al, 2006). A solution's osmolarity is linearly related to its molar concentration, but also increases with its ionicity. Non-ionic CM in comparison with ionic CM, have a lower osmotic load and lack electric charge (Speck, 1999). Furthermore, the toxic effects of high osmolar CM are more intense than the effects of low- or iso-osmolar CM (Haller, Hizok, 2004).

High osmolar iodinated agents represent the first generation of contrast- media. Despite their good opacification they were associated with pseudoallergic reactions and high risk of nephrotoxicity in patients at risk (Tumlin et al, 2006). High osmolar agents diminish the deformability of erythrocytes, increasing the cell's stiffness and red blood cells become densely packed in the capillaries. This complicates the flow of red blood cells as it may stop (Persson et al, 2005). Several studies indicate, though, that adverse effects of high osmolar contrast media may rely on their electric charge rather than their high osmolality (Sendeski, 2011).

The next generation compounds were *low-osmolar* contrast- media that had an osmolarity 2-3 times lower than the high- osmolar ones. Even though they were a significant improvement, their osmolarity was still higher than that of plasma and were associated with contrast- induced nephropathy, in a lower percentage than the previous category (Tumlin et al, 2006). Finally, iso-osmolar contrast-media were produced with an osmolarity of 290 mOsm/kg H_2O (Geenen et al, 2013).

Viscosity is a very important physicochemical parameter, as it is inversely related to osmolarity (Romano et al, 2008). After intravenous injection, fluids with a high viscosity can influence local circulation on a greater degree than those with lower viscosity (Geenen et al, 2013). High viscous contrast media diminish renal medullary blood flow, erythrocyte concentration and pO_2. Recent data from animal studies suggest that iso-osmolar non-ionic dimers compared with low-osmolar non-ionic monomers significantly increase urine viscosity, lead to increased kidney iodine retention and increase the formation of vacuoles in the renal tubular epithelium of the cortex predominantly in the proximal and distal tubulus (called "osmotic nephrosis") (Lenhard et al, 2013).

1.3 Pharmacokinetic properties

After intravenous administration, contrast media are distributed quickly through intravascular and extracellular fluids and have a short distribution half-life (t½d). Usually, the duration for CM distribution over the fluids ranges from 2 to 30 min. Binding with plasma protein is about 1-3 % (Speck, 1999).

Contrast media is not metabolized in mammalian body, but excreted, mostly, via glomerular filtration by the kidneys. The vast majority of contrast media volume, almost 100% is excreted within the first 24 hours in patients with a normal renal function, compared to those with renal function impairment, whose elimination half-life can increase up to 40 hours or more. There are other routes of elimination such as the biliary route, but are relatively slow. If the removal of contrast-media is desirable, haemodialysis and peritoneal dialysis are effective ways for blood clearance (Thomsen et al, 2008). Since more than 95% of an intravascularly administered contrast- media is excreted by the kidneys, it is clear why this is the target organ for contrast- induced toxicity (Rudnick et al, 1994).

1.4 Pathophysiological mechanisms

The pathophysiology of CIN is not completely understood, but it certainly comes as the combination of more than one factors. We can only speculate what happens inside a

human kidney, through the extrapolation of animal and laboratory studies (Remy et al, 2013).

There are numerous in vitro and in vivo studies that have contributed to our knowledge on the condition (Tumlin et al, 2006). Proximal and distal tubular injury occurs at the moment of contact with contrast media and is thought to happen due to the combination of direct tubular cell death, intrarenal vasoconstriction and medullary hypoxia. Renal blood flow is reduced which leads to localized renal ischemia (Barreto, 2007, Sterling et al, 2008, Thomson et al, 2009, Persson et al, 2005). Recently, these findings were confirmed using magnetic resonance imaging (MRI), suggesting the usefulness of this tool in everyday clinical practice (Zhang Y, 2012, Zhang YD, 2014).

In vitro and in vivo experiments lead to the assumption that renal hypoxia enhances ROS formation within the kidney (Pisani et al, 2013). Research has shown the protective role of antioxidant compounds against renal injury which leads to the speculation that free radicals might be involved in the pathophysiology (Romano et al, 2008).

Ischemic injury is thought as a primary mechanism of CIN, and is caused by three pathways*: haemodynamic alterations*, *ROS production* and *direct tubular toxicity*.

1.4.1. Haemodynamic alterations

Under normal conditions, 25% of the cardiac output is directed towards the kidneys. Most of that is headed towards the cortex, leaving the medullary blood flow significantly low. Under physiological circumstances, the medullary part of the kidney is at the verge of hypoxia and regional PO_2 levels can be as low as 20 mmHg, leaving this area more susceptible to fluctuations in oxygen levels (Heyman et al, 1999, Persson, 2005). Outer medulla is the most susceptible part of the medulla, as it contains the metabolically active thick ascending limbs of the loop of Henle. There, the active reabsorption of sodium demands a huge amount of oxygen (Brezis, Rozen, 1995). The reduction of medullary blood flow that occurs during administration of contrast media compromises that delicate balance between oxygen consumption and tissue oxygen availability (Solomon, 2009).

Intraarterial infusion of contrast agents in animals shows a biphasic haemodynamic response: initial vasodilation (with a transient increase in renal plasma flow, glomelular filtration and urinary output) is followed by a prolonged vasoconstriction, resulting in a decline of PO_2 by 50-67%, to 9-15mmHg. The mechanism of this phenomenon is not completely understood, but a research highlighted the importance of calcium influx in the vasoconstriction that follows contrast- media administration (Thomson et al, 2009). More specifically *Bakris and colleagues* showed than with a pretreatment of a canine model with T- type calcium channel blockers (diltiazem or veparamil) or ethylene glycol tetraacetic acid (EGTA), a nonspecific calcium chelator, the vasoconstriction was markedly attenuated (Bakris et Burnett, 1985).

The vasoconstrictive phenomena are also thought to be caused by the imbalance of various vasoactive substances, such as endothelin, adenosine and nitric oxide (NO) (Thomson et al, 2009). Contrast agents may provoke the release of endothelin and adenosine from endothelial cells, thereby increasing vasoconstriction, and decrease the release of prostaglandins and NO, which are vasodilators (Nugan, Brogan, 2009, Persson, 2005). *Ribeiro and colleagues* compared contrast agents of different osmolarities and showed that the reduction of NO production was proportional to the osmolarity of the contrast media in vitro, in cultured muscle cells from the renal artery. This showed that, apart from the direct vasoconstriction of renal vasculature, iodinated contrast- media block an important pathway for vasodilation and autoregulation (Ribeiro et al, 2004). Medullary hypoxia is a combination of a reduction in microcirculatory blood flow and increased oxygen demand of tubular cells (Heyman et al, 2008).

1.4.2 Reactive Oxygen Species

Free radicals are atoms or molecules that contain one or more unpaired electrons. These molecules are changed into water after reduction reactions. Less aggressively reacting molecules such as H_2O_2 are called reactive oxygen species (ROS) (Katzberg, 2005). Under normal circumstances, tubular transport is associated with ROS formation, mostly in thick ascending limb, where, superoxide anions ($O2^-$) and hydroxyl radicals (OH^-) are produced by NAD(P)H- oxidase in mitochondria (Heyman et al, 2010). ROS play an important role in cellular signaling processes, regulation of regional microcirculation (through its effects in NO levels) and tubular transport activity. Tissue

injury can take place when the amount of ROS exceeds the antioxidant capacity of the organism.

Contrast media- administration, significantly decreases medullary oxygenation, but reabsorption in medullary area remains the same (Pisani et al, 2013). ROS increase two vasoconstrictive agents, angiotensin- II and endothelin-I (through the activation of endothelin- converting enzyme-1(Pisani et al, 2013)), and reduce the bioavailability of the vasodilative NO (Heyman et al, 2010). The intense vasoconstriction with the loss of autoregulation may lead to a depressed activity of mitochondrial scavengers and augmented release of reactive oxygen species (ROS). During hypoxia, ATP is converted to ADP and AMP, which in turn are metabolized to adenosine and finally to hypoxanthine, that uses the enzyme *xanthine oxidase* to convert to xanthine and hydrogen peroxide. Xanthine uses also this enzyme to produce uric acid and more hydrogen peroxide that scavenge NO (Pisani et al, 2013). Normally, NO prevents ROS-mediated endothelial cell injury and reduces transport-dependent ROS formation in medullary thick ascending limbs. Superoxide radicals react with NO, reducing its bioavailability and producing peroxynitrite, an oxidative and very reactive nitrosative species that provokes endothelial dysfunction, further tissue impairment (Detrenis et al, 2005, Pisani et al, 2013).

Impairment in flow leads to medullary hypoxia and decreased nutrient delivery to tubular epithelial cells, increases ROS formation, resulting in breakdown of the epithelial cytostructure, causes lipid peroxidation shown by increased malondialdehyde (MDA) levels (Detrenis et al, 2005) with loss of cell balance and cell death (Choudhury, 2010, Nugan, Brogan, 2009).

1.4.3 Direct tubular toxicity

Direct effects of CM should better be studied in vitro, in order to exclude the other mechanisms of injury such as hypoxia and, indeed, cell culture studies have shown the direct cytotoxic effects of iodinated contrast media on a variety of cell lines (Heinrich et al, 2005). Some of the mechanisms described are: generation of ROS (Detrenis et al, 2005, Heinrich et al, 2005, Persson et al, 2005), redistribution of membrane proteins, altered mitochondrial function, reduction of extracellular Ca^{+2}, DNA fragmentation, disruption of intracellular junctions, reduced cell proliferation, and apoptosis (Haller, Hizok, 2004). Cytotoxic effects of CM on glomerular mesangial cells include apoptotic

effects, associated with elevated ROS levels, which shows the interaction between CIN pathophysiological mechanisms (Haller, Hizok, 2004).

Contrast media induced acute kidney injury is associated with tubular damage either due to direct tubular injury or renal ischemia. The impairment is located mainly in proximal tubular epithelium. The typical lesions range from tubular vacuolation to tubular necrosis of proximal tubular epithelium, accompanied with proteinaceous casts in the medullary ducts, as shown in research studies. However, the glomeruli remain intact (Buyuklu et al, 2015, Ari et al, 2012, Ozkan et al, 2012, Hsu et al 2009).

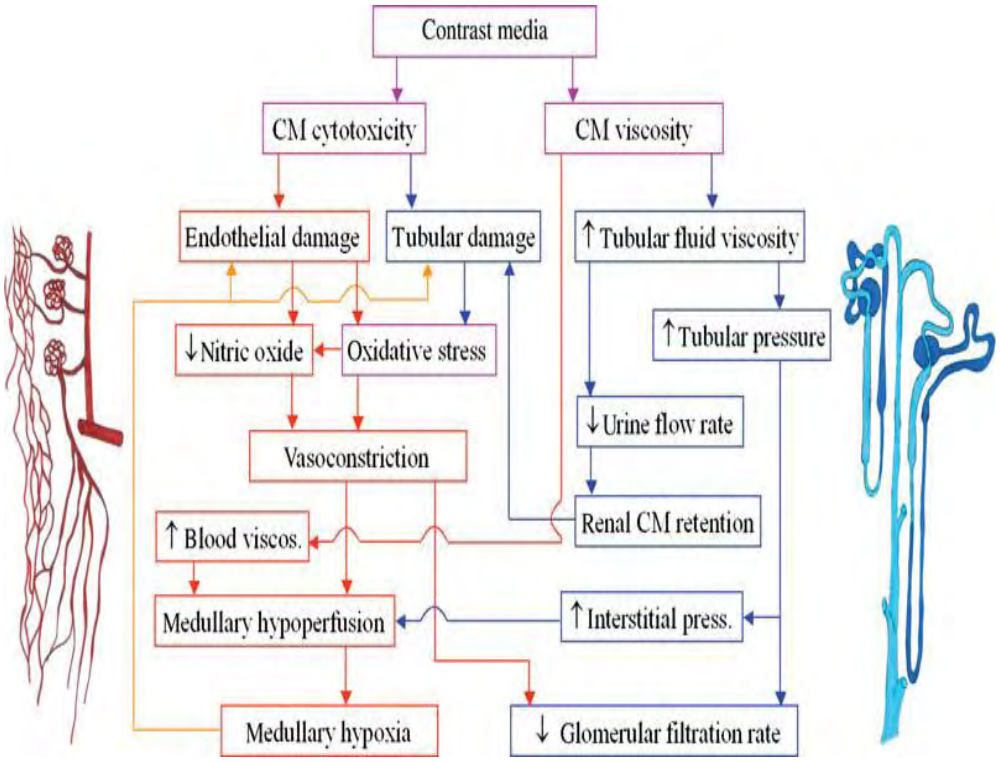

Figure 4: Simplified scheme portraying the main pathophysiological mechanisms of CIN

1.4.4 Apoptosis

Aς far as *apoptosis* is concerned, it is a form of programmed cell death that occurs as a physiological mechanism, during development and aging, to maintain homeostasis but also, as a defense mechanism such as in immune reactions or when cell populations are damaged due to drugs, infectious or toxic agents (Norbury, Hickson, 2001).

There are two main apoptotic pathways: the extrinsic or death receptor pathway and the intrinsic or mitochondrial pathway. However, there is now evidence that the two pathways are linked and that molecules in one pathway can influence the other (Igney, Krammer, 2002).

The extrinsic pathway is initiated by death receptors, members of the tumor-necrosis factor receptor (TNFR) superfamily (Linkermann et al, 2012) and results in the expression of ligands for phagocytic cell receptors and finally uptake by phagocytic cells (Martinvalet et al., 2005). In the intrinsic pathway, which is independent of death receptors (Linkermann et al, 2012), stimuli cause changes in the inner mitochondrial membrane that result in an opening of the mitochondrial permeability transition (MPT) pore, loss of the mitochondrial transmembrane potential and release pro-apoptotic proteins into the cytosol, such as cytochrome c (Saelens et al., 2004). Both pathways end at the execution phase, considered the final pathway of apoptosis, where the execution caspases that begin this phase of apoptosis are activated. Caspase-3 is considered to be the most important of the executioner caspases and is activated by any of the initiator caspases (caspase-8, caspase-9, or caspase-10) (Slee et al., 2001).

Apoptotic cells are characterized by cellular shrinkage (puknosis), nuclear and cytoplasmic condensation, nuclear fragmentation (karryorhexis), plasma membrane blebbing, vacuoles containing cytoplasmic portions and fragment in discrete corpses (known as apoptotic bodies) (Linkermann et al, 2012).

There is plenty of research showing that apoptotic cell death is a prominent and characteristic feature of acute kidney injury provoked by intravenous contrast agents, in vitro (Huang et al, 2015, Romano et al, 2008) and in vivo (Liu et al, 2014, Ozkan et al, 2012, Lee et al, 2011, Zhao et al, 2011, Hsu et al, 2010). Recently an in vitro and in vivo assessment of pathways involved in CIN, portrayed apoptosis as a key mechanism of CIN. More specifically, apoptotic cell death was provoked by three pathways: ROS pathway, stress kinase pathway and intrinsic apoptotic pathway (Quintavalle et al, 2011). However there is recent research data that question the role of apoptotic cell death in CIN (Linkermann et al, 2013).

1.4.5 Necroptosis

For a long period of time, it was believed that apoptosis was the only form of cell death responsible for acute kidney injury (Havasi, 2011). However, potential therapeutic anti-apoptotic interventions showed efficacy only in animal models and not in clinical conditions. Research progress characterize other forms of cell death to be implicated in the pathogenesis of CIN, too, with necroptosis been more extensively studied in acute kidney injury (Linkermann et al, 2014). Necroptosis is a programmed form of necrosis, with morphologic features of necrosis but molecularly controlled (Wang et al, 2006). It was introduced in 2005, when *Degterev and colleagues* identified necrostatin-1 (Nec-1) which is an inhibitor of necroptosis (Degterev et al, 2005). Necrotic phenomena can be initiated by the engagement of death receptors, Toll- like receptors (TLRs) and interferon signals and are highly dependent on receptor- interacting protein kinase 3 (RIP-3) and lineage kinase domain- like protein (MLKL) (Linkermann, Green, 2014).

Necroptosis was recently associated with CIN (Linkermann et al, 2012). Linkermann and colleagues showed that contrast- media induced renal insult was almost totally prevented in Nec-1 treated mice (Linkermann et al, 2013). *Liang and colleagues* reported that necroptosis contributed to CIN in an ATP-depleted model (Liang et al, 2014). However, *Huang and colleagues* in an in vitro study in human renal proximal tubule epithelial cell line (HK-2) showed that necrosis and not necroptosis occurred, as there were not any changes in RIP3 expression and Nec-1 did not reduce the observed cytotoxicity (Huang et al, 2015). Better understanding of the necroptotic pathway may lead to new preventive strategies for CIN (Wang et al, 2016).

1.4.6 Renal efferent nerve activity

A very interesting mechanism, is the role of renal efferent nerve activity (RENA). Physiology suggests that activation of RENA provokes vasoconstriction, raises RVR and increases renin from juxtaglomerular granular cells. Renin release increases angiotensin activity which sequentially releases aldosterone, and this mechanism further aggravates vasoconstriction and increases ROS production (Wang et al, 2003). Shih- Ping et al, demonstrated that renal denervation ameliorated ROS production, vacuole formation and apoptosis phenomena caused by the ionic and high osmolar CM, ioxitalamate. They proved that RENA is a crucial mechanism of CM- induced acute kidney injury (Shih- Ping et al, 2010).

The clarification of the factors affecting renal microcirculatory hemodynamics is pivotal to understanding the pathogenesis of CIN and the expected response to preventive measures.

1.5 Risk factors

There are specific risk factors that predispose to CIN. The most significant risk factor is the preexisting renal impairment (Barrett, Parfrey, 2006). More specifically, patients with estimated glomerular filtration rate (eGFR) less than 60mL/min/1.73 m^2 before intra-arterial and eGFR less than 45 mL/min/1.73 m^2 before intravenous administration are in risk for CIN (Thomsen, Webb, 2014). The antioxidant mechanisms of patients with chronic renal failure are impaired and they show increased oxidative stress derived from inflammation and endothelial dysfunction (Martin-Mateo, 1999, Okamura, 2009). It is generally admitted that the higher the contrast medium dose and the lower the glomerular filtration rate (GFR) the higher the risk for a patient to develop nephropathy (Petterson et al, 2002).

The volume of contrast media was an ambiguous risk factor for years, as there was believed to be a correlation between contrast volume and risk of CIN. Studies showed that CIN increased proportionally to the doses of contrast media (Rosovsky et al, 1996, Kane et al, 2008) and ROS production seemed to be significantly proportionate to it (Fiaccadori et al, 2004). In recent meta-analysis, though, contrast volume does not appear to have a significant association with CIN incidence (Moos et al, 2013).

Diabetes mellitus is a very important predisposing factors for CIN, as diabetic patients with CIN have a decreased survival rate than non-diabetic patients over a 2-year follow-up (Zaytseva, 2009). Ionic contrast media induced more apoptosis in diabetic kidneys than nonionic contrast media (Hsiang-Lee et al, 2011). A potential mechanism of action would suggest that glucose aggravates the oxidative stress caused by CM in mesangial cells, regardless of its osmotic effect (Wasaki et al, 2001). Furthermore, patients with both diabetes and renal failure are at a high risk for CIN, due to a reduction in NO and prostaglandins, endogenous vasodilators, that results in a decrease in GFR and renal blood flow (Sterling et al, 2008, Thomson et al, 2009). In a recent large scale study among patients with acute- myocardial infarction that underwent coronary angiography, it was shown that pre-procedural elevated glycose levels increased risk

for CIN even though these patients were not diagnosed as diabetic patients (Stolker et al, 2010).

The patient's age, is a factor that should be taken into consideration, as it is accompanied with reduced renal mass, function and perfusion. Other factors that result in renal hypoperfusion such as cardiovascular disease, hypotension and cirrhosis are most likely to predispose to CIN. Renal injury may also be provoked by sepsis through the release of bacterial toxins towards renal tubules (Gupta et al, 2010). Multiple contrast induced administrations within a few days are not recommended, as they are involved in increased risk (Thomsen, Webb, 2014).

High osmolar CM have shown an increased risk of CIN in comparison with iso- or low-osmolar ones, as well as intra-arterial compared to intravascular administration (Gupta et al, 2010). A large-scale review of papers from 1996 to April 2010 was performed from the *Contrast Media Safety Committee of the European Society of Urogenital Radiology* to compare the risk after intra-venous and intra-arterial administration of contrast-media. The results showed that intra-venous route was safer than the intra-arterial (Stacul et al, 2011). An explanation would be that contrast-medium that travel through the arteries reaches kidneys more quickly and dilutes minimally whereas the intravenous route requires smaller amounts of contrast media and the contrast agent is diluted in the circulation before reaching renal vasculature (McCullough, 2008, Caiazza et al, 2014). However, the research outcomes are contradictory on this risk factor, as a recent study showed a slight, non-significant, increase of CIN incidence in intra- arterial rather than intravenous administration (14% and 11, 7 % respectively) after adjustment for patient- related risk factors (Kooiman et al, 2013).

Systemic inflammation is an interesting factor, as studies show that elevated pre-procedural C-reactive protein was a strong and independent predictor of CIN (Evola et al 2012), and the administration of statins- whose beneficial role in systemic inflammation is well clarified- was associated with reduced incidence of CIN (Patti et al, 2008, Xinway et al, 2009). In addition, when the degree of systemic inflammation increased, the number of affected vessels increased, linking CRP to atherosclerotic disease (Rizzo et al, 2009), but a direct correlation between sick vessels and CIN could not be proven (Evola et al 2012). Nevertheless, studies suggest that extracoronary atherosclerosis may be another risk factor of CIN, as a link between cardiovascular and

renal disease (Kowalczyk et al, 2007). Systemic inflammation, of which atherosclerosis is an expression, may provoke alterations in the renal microcirculation, predisposing to CIN (Evola et al, 2012).

2. The aim of the study

This study aimed to contribute to the understanding of the pathophysiological mechanisms of contrast- induced nephropathy through the rabbit nephrotoxicity model. For this reason, 9 male New Zealand White rabbits were used divided into three groups: i) *24-hour CIN group* (n=3) which was euthanized in 24 hours after CM administration, ii) *48-hour CIN group* (n=3) and iii) *Control group* (n=3) which were euthanized in 48 hours after CM and normal saline administration respectively. Blood collection was performed at 2h, 10h 24h and 48 h (for Control and 48h CIN group) after CM administration. Histopathological examination of the kidneys was performed using different dyes that portray specific structures of the kidney. The renal abnormalities were correlated with the oxidation- reduction status in three separate kidney areas (cortex, juxtamedullary, medullary regions), which was evaluated via oxidative stress biomarkers. Finally, the apoptotic pathway was examined with the appropriate kit.

3. Experimental protocol

Rabbit model of contrast induced nephropathy

Although CIN is mostly studied in rat models, this is not the ideal model, as CIN cannot be provoked in normal animals (Aspelin et al, 2003). Most researches induced prerenal azotemia via 16-24 hour water deprivation (Zhao et al, 2011, De Almeida et al, 2016, Buyukly et al, 2015, Ozkan et al, 2011) or even by removing a large part of the animal's kidneys accompanied by 48-hour water deprivation (Tong-qiang et al, 2014). Some researchers even treated rats with nephrotoxic drugs or with a combination of substances that provoked nephrotoxicity (Kiss et al, 2016).

New Zealand White rabbit was chosen as the experimental model (Pettersson et al, 2002, Lauver, 2014). Although morphologically the rabbit resembles to rodents, protein sequence data suggest that rabbits are more closely related to primates than rodents (Graur et al, 1996), their renal function is known to be sensitive to contrast

agents (Golman, 1984), and comparative studies have shown that the rabbit model is more sensitive to contrast agents than the rat (Bhargava et al, 1990). More specifically, New Zealand white rabbits are known to be more susceptible to CIN (Lauver et al, 2014). CIN can be provoked in normal *rabbits*, with a single injection of iodinated contrast media and for all these reasons rabbits represent a more reliable model of nephrotoxicity (Kiss et al, 2016).

Nine male New Zealand white rabbits (5-6 months old and weighing approximately 3,5 kg) were housed in standard conditions with access to standard rabbit food and tap water *ad libitum*. The animals were randomized and divided into three groups in the beginning of the study: i) *24-hour CIN group* (n=3), ii) *48-hour CIN group* (n=3), iii) *Control group* (n=3). The CIN model was developed on the basis of previously described rabbit renal toxicity test (Petterson et al, 2002) and involved intravascular administration of the non- ionic, low- osmolar iodinated contrast agent iopromide (Ultravist®, Bayer Healthcare, Berlin, Germany), at the dose of 8g/kg iodine through the rabbit's marginal ear vein over a period of 30 minutes. At the beginning of each administration, the animals were weighed and anaesthetized by intramuscular administration of Xylazine (Xylapan®, 4 mg/kg) and Ketamine (Narketan®, 40mg/kg) before the administration of iopromide. A cannula was placed in a marginal ear vein for the administration of contrast agent. Blood collection was performed at 2h, 10h, 24h and 48h after contrast-media administration. The animals were euthanized with IV infusion of Pentobarbital Sodium (Dolethal®, 5 ml per animal) at 24 hours (24-hour CIN group) and 48 hours (48-hour CIN group and Control group). Right after their death, all the animals were weighted and the kidneys were explanted with the standard necrotomy procedure. The left kidneys were sliced longitudinally and the right kidneys transversely.

3.1 Renal function evaluation

Blood samples were collected in plain tubes, centrifuged at 1500 g for 10 minutes and serums were extracted. Serum urea and creatinine concentrations were analyzed by a standard spectrophotometric assay COBAS INTEGRA® 400 plus analyzer, Roche.

3.1.1. Serum Urea

Urea is the primary nitrogenous waste product of metabolism generated from tissue protein turnovers and dietary protein degradation. It is eliminated almost exclusively by the kidneys and can be measured in the urine and blood as a marker of renal function. The higher urea levels represent the lower excretion from the kidney due to renal impairment (Walker et al, 1990). For the rabbit, the normal range in blood serum is 5-25 mg/dL (Suckow and Schroeder, 2010). This wide range depends on many factors, such as state of hydration, protein intake, endogenous protein catabolism, hepatic urea synthesis and renal urea excretion (Walker et al, 1990).

3.1.2. Serum Creatinine

Creatinine is the product of muscle creatine catabolism. Normal kidneys filter creatinine and the latter is excreted from the body. Renal impairment leads to increased creatinine levels in blood and urine. The normal serum creatinine values vary, depending on the patient's mucle mass (Walker et al, 1990). As far as the adult rabbit is concerned, the range is 0,5-2,6 mg/dL (Suckow and Schroeder, 2010).

3.2 Oxidative stress biomarkers

Samples from the left kidney were preserved in -80 ^{o}C for the assessment of oxidation reduction biomarkers. ROS production differences were examined separately in renal cortex, juxtamedullary and medullary area, as it is widely known that there are differences in oxygen pressure in these three different parts of the kidney. Kidney cortex receives adequate blood volume, whereas partial oxygen pressure in corticomedullary junction declines from 20- 30 mm Hg to 15 mm, accompanied by hypoxic tubular injury (Haschek et al, 2013, Liss P et al, 1998) and as mentioned above, ischemic phenomena occur in medullary area. It should be highlighted that, as the rabbit's kidneys consist of a single lobe (unipyramidal) there is clear distinction of these three parts of the kidney (Dimitrov et al, 2012).

Before all measurements it was essential to perform tissue homogenization. For this reason one part of tissue specimens was homogenized with two parts of Phosphate Buffer Saline (PBS) (pH=7, 4, 138 mM NaCL, 2,7 mM KCL and 1 mM EDTA,) and protease inhibitor tablet (Complete Mini Protease Inhibitor Cocktail Tablets - Roche Diagnostics GmbH). The homogenate was vigorously vortexed and a brief sonication

treatment on ice was applied, so as to release the maximum protein amount possible, and was centrifuged in 15.000 g for 5 minutes in 4^{o} C. The supernatant was collected in eppendorfs tubes, stored at -80^{o} C and this was the sample used for all the oxidative stress biomarkers.

3.1.1. Bradford Protein Assay

The Bradford protein assay is a spectroscopic analytical procedure used to determine the total protein concentration of a sample. The method is based on the fact that, interaction of "Coomassie Brilliant Blue G-250" dye of Bradford reagent with amino-acids, turns its colour from red to blue and its absorbance from 365 to 595 nm. The protein concentration of a test sample is determined by comparison to that of a series of protein standards known to reproducibly exhibit a linear absorbance profile in this assay *(Bradford, 1976)*.

In order to make the curve of albumin, successive dilutions of albumin solution of 10 mg/mL were performed, to achieve the final concentrations of 25, 50, 100, 200, 400, 800 and 1000 μg/mL. Then, 1 mL of Bradford reagent was added to 20 μL solution of albumin of each of the concentrations mentioned above. For the blank 20μL H_2O and 1 mL of Bradford reagent were used. The samples were stirred gently, and incubated for 15 min at room temperature until colour stabilizing. The absorbance was measured at 595 nm. The concentrations of albumin correspond to the linear part of the curve. The photometer is resetted in plain air.

3.1.2. Catalase

Catalase (CAT) is an antioxidant enzyme which is present in most aerobic cells. It is involved in the detoxification of hydrogen peroxide (H_2O_2), a type of ROS which is a toxic product of both aerobic metabolism and pathogenic ROS production. The enzyme catalyzes the conversion of two molecules of H_2O_2 to molecular oxygen and two molecules of water (catalytic activity), as seen at the equation that follows:

$$2\ H_2O_2 \rightarrow O_2 + 2\ H_2O$$

Catalase also demonstrates peroxidatic activity, in which low molecular weight can serve as electron donors. While aliphatic alcohols serve as specific substrates for CAT, other enzymes with peroxidatic activity do not utilize these substrates. Catalase is measured via spectrophotometry, by measuring the absorbance at 240 nm for 130 seconds.

The reagents used, were ***Phosphate buffer (KH_2PO_4 + Na_2HPO_4)*** *and* ***Hydrogen peroxide***

- Phosphate buffer 67 mM (pH 7.4)

In order to make 500 mL of phosphate buffer, 100 mL KH_2PO_4 (67 mM) and 400 mL Na_2HPO_4 (67 mM) were prepared. For KH_2PO_4, 0.91 g were weighted and dissolved in 100 mL water (this solution has initial pH ~4.57). For Na_2HPO_4, 4.77 g were weighted and dissolved in 400 mL water (this solution has initial pH ~9.11). In a heating glass the 400 Na_2HPO_4 and the KH_2PO_4 solutions were mixed. If required, the pH was corrected with NaOH or HCl, 1 N, until 7.4.

- 30% hydrogen peroxide (H_2O_2)

Hydrogen peroxide was ready to use.

Assay

The following volumes were added in plastic tubes:

	Sample
Phosphate buffer 67 mM, pH 7.4	2945 μL
Tissue sample	50 μL

Table 1 : Catalase procedure

Firstly, the tubes were vortexed at a moderate speed and then incubated in the oven at 37 ºC for 10 min. Generally, it is more practical to work with 2 samples at a time to make sure that the samples are measured shortly after the incubation. Then, the content

of each plastic tube was transferred into the UV glass cuvette. Finally, 5 μL of 30% hydrogen peroxide were added into the UV glass cuvette, the cuvette was inverted three times (using a parafilm plastic piece on the top of cuvette), and the absorbance was measured immediately at 240 nm for 130 sec. Each sample was preceded separately.

Calculations

Catalase activity (mmol/L/min) = $\Delta Abs_{sample} - \Delta A_{blank}$ (min) / 40 × 60 × 10^3, where 60x10^3 is the dilution factor which results by dividing the final volume (3000 μL) to sample volume (50 μL) (3000 / 50 = 60) and then it is multiplied by 1000 in order to convert mmol/mL to μmol/mL. 40 (mol/L) is the molar extinction coefficient* of H_2O_2.

Δ Abs (min) = the change in absorbance in a min. The concentration of H_2O_2 in cuvette is about 16 mM.

*The molar extinction coefficient of a substance is the absorbance of this substance at concentration 1 mol/L. (Aebi, 1984)

3.1.3. Total Antioxidant Capacity

The term Total Antioxidant Capacity (TAC) is referred to the capability of the tissue components to scavenge reactive species. It is an indicator of the overall antioxidant capacity of a tissue.

There are two different ways of approaching the quantification of antioxidant activity. The first is the sum of the antioxidant capacity of the individual antioxidants of the tissue. This is a very difficult effort and the results will not be accurate as there are a lot of molecules that contribute to the antioxidant capability of each tissue. The second one is the measurement of the total capacity as a whole that provide an overview of the biological interactions between antioxidant species.

Total Antioxidant Capacity of a tissue is evaluated using the 1,1-diphenyl-2-picrylhydrazyl (DPPH). In the presence of a hydrogen donor existing, the free radical DPPH• is reduced to the corresponding hydrazine. The depletion of the radical is photometrically evaluated by the decrease in absorbance at 520 nm.

The reagents used were ***Phosphate buffer (*** $\boldsymbol{KH_2PO_4}$ + $\boldsymbol{Na_2HPO_4}$**)** and ***DPPH.***

- Phosphate buffer 10 mM (pH 7.4)

In order to make 500 mL of phosphate buffer, 100 mL KH_2PO_4 (10 mM) and 400 mL Na_2HPO_4 (10 mM) were prepared. For KH_2PO_4, 0.136 g were weighted and dissolved in 100 mL water (this solution has initial pH ~4.57). For Na_2HPO_4, 0.712 g were weighted and dissolved in 400 mL water (this solution has initial pH ~9.11). In a heating glass the 400 mL of Na_2HPO_4 and the 100 mL of KH_2PO_4 solutions were mixed. If required, a correction was made with NaOH or HCl, 1 N, until pH 7.4.

- DPPH (2, 2-diphenyl-1 picryl hydrazyl) 0.1 mM. MW (DPPH): 394.320.02

DPPH were dispensed in 5 mL methanol and the solution was mixed in the stirrer (10 mM solution). Then, 100 times dilution was made with methanol and mixed in the stirrer, for example, 200 μL of the 10 mM DPPH solution were diluted into 19.8 mL methanol (enough for 10 samples, plus the Blank and the Positive Control). Due to the dilution, the initial volume of 5 mL is always enough for the determinations. The solution is highly photosensitive. DPPH is made fresh in the day of the experiment.

The following volumes were added in eppendorf tubes:

	Blank	*Sample*
Phosphate buffer 10 mM, pH 7.4	*500 μL*	*450 μL*
DPPH 0.1 mM	*500 μL*	*500 μL*
Tissue sample	—	*50 μL*

Table 2 : TAC procedure

The eppendorfs were incubated in the dark for 60 min and then centrifuged for 3 min at 20000 g at 25 ^oC in the eppendorf centrifuge. At last, 900 mL of the supernatant were

transferred using pipet from each eppendorf into a plastic cuvette and measured the absorbance at 520 nm.

Calculations

Results can be expressed as:

i) % absorbance reduction (Abs) in reference to blank, ie,

% Abs reduction = (Abs blank – Abs sample) / Abs blank × 100

ii) μmol DPPH scavenged / mL sample = [(% Abs reduction / 100) × 50 × 50] / 1000

α) We divide by 100 in order to convert percentage absorbance decrease into absorbance decrease.

β) We multiply by 50 because the concentration of DPPH in the cuvette is 50 μmol/L of the cuvette.

γ) We multiply by 20 because dilution of the serum in the cuvette is 20-fold (1000 μL in the cuvette / 50 μL sample in the cuvette = 20).

δ) We divide by 1000 in order to convert the L of sample to mL of sample.

Example. If the % absorbance reduction is 20, the μmol DPPH scavenged/ mL sample are: 20/ 100 × 50 × 20 / 1000 = 0.2 μmol DPPH scavenged / mL sample or 0.2 mmol DPPH scavenged / L sample ή 0.2 mmol DPPH/L. (Janaszewska & Bartosz, 2002)

3.1.4. Protein Carbonyls

Proteins in general and amino acids are susceptible to oxidative damage. Protein carbonyls (PC) are generic markers of oxidation and frequently utilized. They are indices of protein oxidation in general and probably more reliable ones. CO (carbonyl groups such as aldehydes and ketones) are produced on protein side chain of Proline, Arginine, Lysine and Threonine mainly. They are preferable markers and one reason for this is the fact that they are stable moieties.

Carbonylated proteins are irreversibly damaged. The carbonylation leads to the loss of their physiological function. The moderately carbonylated proteins are degraded by the proteasome but if they are severely damaged, they cannot be degraded and are accumulated forming high-molecular weight aggregates. Protein oxidative damage not only affects their function but also the interaction with other biomolecules. For example, if DNA repair enzymes or DNA polymerases undergo carbonylation or other form of oxidative damage, DNA will not be repaired or replicated following the necessary fidelity.

Carbonyl formation is usually detected by a reaction with 2, 4- dinitrophenylhydrazine (DNPH) and the conversion to 2,4-dinitrophenylhydrazone (DNP-hydrazone).

*The reagents used were **TCA**, **HCl**, **DNPH** and **Urea**.*

- TCA is being added to the sample in order for the proteins to be precipitated.

-TCA 10%: For its preparation 10g of TCA were weighted and dissolved in distilled water up to a final volume of 100 mL of water (stable at room temperature).
-TCA 20%: For its preparation 20 g of TCA were weighted and dissolved in distilled water up to a final volume of 100 mL of water (stable at room temperature).

- *HCl 2.5 N*

In order to make 100 mL of 2.5 N HCl solution, 24.6 mL of 37% HCl (it is equal to 10.1 N HCl) were slowly added to ≈70 mL water and then added more to reach the final volume of 100 mL of water.

- *DNPH 14 mM*

In order to make 100 mL of 14 mM DNPH 0.2833 g DNPH were diluted in 100 mL 2.5 N HCl. This dilution is always made the day of the experiment and is photosensitive.

- *Urea 5 M (pH 2.3)*

Urea, is a powerful protein denaturant. This property can be exploited to increase the solubility of proteins. Urea effectively disrupts the noncovalent bonds in proteins

In order to make 100 mL of 5 M Urea (pH 2.3, 2N HCl), 30 g Urea were diluted in ≈70 mL water and then added more water to the final volume of 100 mL.

Assay

In 50 μL of sample, 50 μL 20% TCA were added in eppendorf tubes and vortexed. Every sample has a positive blank. Incubation in ice bath for 15 min was performed and then the samples were centrifuged at 15,000 g for 5 min at 4 ^{o}C. Afterwards, the supernatant was discarded and then 0.5 mL of 14 mM DNPH (in 2.5 N HCL) were added in the pellet for the sample and 0.5 mL 2.5 N HCL for the blank, the pellet was manually suspended using pipette tip, vortexed and incubated in the dark at room temperature for 1 h. Intermittent vortexing was performed every 15 min. Centrifuged at 15,000 g for 5 min at 4 ^{o}C, and then the supernatant was discarded. 1 mL of 10% TCA was added, vortexed and centrifuged at 15,000 g for 5 min at 4 ^{o}C. Then the supernatant was discarded and 0.5 mL ethanol and 0.5 mL ethyl acetate (ethanol/ethyl acetate, 1:1 v/v) were added, vortexed and centrifuged at 15,000 × g for 5 min at 4 ^{o}C. The pellets were washed with 10% TCA followed by three ethanol–ethylacetate (1:1) (v/v) washes to remove any unreacted DNPH.

Following, the supernatant was discarded, 1 mL 5 M Urea (pH 2.3) was added, vortexed and incubated at 37 ^{o}C for 15 min. Then, it was centrifuged at 15,000 g for 3 min at 4 ^{o}C, transferred by pipette 900 mL into a cuvette and measured the absorbance at 375 nm.

Calculations

Protein carbonyl calculation is:

Protein carbonyls (nmol/mL) = A_{sample} - A_{blank} / 0.022 × 1000/50.

The molar extinction coefficient* of DNPH is 22 mM · cm^{-1}.

0.022 is calculated as follows: 22 mmol/L equals to 22 μmol/ml, equals 0.022 nmol/ml. Where 1000 / 50 is the dilution factor (1000 μl in the cuvette/50 μl of the sample),

Normalization for protein concentration can be done by the following formula:

Protein carbonyls (nmol/mg) = carbonyl conc. nmol/mL / protein conc. mg/mL

Protein concentration = 70 mg/mL.

*The molar extinction coefficient of a substance is the absorbance of this substance at concentration 1 mol/L (Patsoukis et al, 2004).

3.1.5. TBARS

Oxidative stress in the cellular environment results in the formation of highly reactive and unstable lipid hydroperoxides. Malondialdehyde (MDA) and 'Thiobarbituric Acid Reactive Substances' (TBARS) are end products of lipid peroxidation of membrane polyunsaturated fatty acids by free radicals and are indicators of oxidative damage. Administration of contrast media leads to an increase of renal tissue and serum MDA levels and renal tissue TBARS on experimental CIN models (Devrim et al, 2009).

The measurement of TBARS is a well-established method for screening and monitoring lipid peroxidation. TBARS are expressed in terms of MDA equivalents. MDA forms a 1:2 adduct with Thiobarbituric acid (TBA), which can be measured by spectrophotometry. TBARS return to normal levels over time, depending upon the presence of anti-oxidants. The thiobarbituric acid reactive substances (TBARS) test is a quick and easy way to assess lipid peroxidation as the levels of derivatized Malondialdehyde (MDA). The product is the MDA $(TBA)_2$ adduct, whose absorbance is measured at 530 nm.

*The reagents used were **Tris-HCL**, solution of **Na_2SO_4** – **TBA** and **TCA** of 35% and 70% concentrations.*

- **Tris-HCl** 200 mM (pH 7.4)

Tris is an abbreviation of the trivial name (trishydroxymethylaminomethane) for 2-amino-2-hydroxymethyl-1,3-propanediol. It is widely used as a component of buffer solutions with an effective pH range between 6.5 and 9.7. To make ≈100 mL of Tris-HCl buffer, 25 mL Tris (200 mM) and 42 mL HCl (0.1 N) were prepared. For Tris 0.61 g were weighted and dissolved in 25 mL water. For HCl 0.42 mL of the stock 37% HCl (equal to 10.1 N) were diluted up to 42 mL water. 25 mL of Tris solution were poured in a heating glass, 42 mL HCl were slowly added, and then water was added up to 100 mL. PH measurement was performed to ensure that it was approximately 7, 4.

- Solution **Na_2SO_4** (2 M) – **TBA** (55 mM)

Na_2SO_4 is used as a drying agent for organic solutions. In order to make 10mL of a solution, 2.84 g Na_2SO_4 and 0.08 g TBA were weighted, transferred in a heating glass and 10 mL water were added.

- **TCA** is being added to the sample in order for the proteins to be precipitated.

-TCA 35%: For its preparation, 35 g of TCA were weighted and dissolved in distilled water up to a final volume of 100 mL of water (stable at room temperature).

-TCA 70%: For its preparation, 70 g of TCA were weighted and dissolved in distilled water up to a final volume of 100 mL of water (stable at room temperature).

Assay

Falcon tubes (15 mL) were used, where 100 μL tissue sample was added, or distilled water (for the blank). Then, 500 μL TCA 35% and 500 μL Tris-HCl were added and vortexed, followed by incubation for 10 min at room temperature. 1 mL Na_2SO_4 – TBA was added and incubated at 95 ^oC for 45 min in the waterbath. I transferred the tubes to the ice and let them cool for 5 min. 1 mL TCA 70% was added and vortexed. 1 mL was then transferred into eppendorf tubes and centrifuged at 11200 g (10000 rpm) at 25 ^oC

for 3 min. Finally, 900 μL were transferred by pipette into a cuvette and the absorbance was measured at 530 nm.

Calculations

The concentration of TBARS (μmol/L) = ($Abs_{sample} - Abs_{blank}$) / 0.156 × 7.5, where 7.5 is the dilution factor, which results if dividing the final volume (3000 μL) to the volume of the sample (400 μL) (3000 / 400 = 7.5). To 0.156 results from the molar extinction coefficient* of MDA which is 156000 (mol/L) divided by 10^{-6} in order to convert mol/L to μmol/L. After calculating μmol/L MDA in the samples, the results are coverted to nmol MDA/mg of protein in the corresponding samples.

*The molar extinction coefficient of a substance is the absorbance of this substance at concentration 1 mol/L. (Keles et al, 2001).

3.3 Histopathological evaluation

For histopathological examination, slices from both explanted kidneys were fixed in 10% phosphate- buffered formalin solution overnight. Left kidneys were sectioned longitudinally and right kidneys transversely. Then, automated dehydration followed through a graded ethanol series, transverse kidney slices were embedded in paraffin and 5 μm sections were cut on a rotary microtome. Kidney sections were stained with Hematoxylin Eosin (H &E), Periodic Acid- Schiff (PAS), Masson's Trichrome and Jone's Silver Methenamine stains.

Histopathological changes were analyzed for tubular necrosis, tubular vacuolization and proteinaceous casts. Cortical alterations were graded as follows: 0: no damage, 1: mild (damage less than 25%), 2: moderate (damage between 25 and 50%), 3: severe (damage between 50 and 75%), 4: very severe (more than 75% damage). Light microscope was used to evaluate the sections from an experienced pathologist who was blinded to the data. Photographs were taken at 200x magnification.

The following stains were used, each of them coloring the otherwise transparent tissue sections (2, 3, 5):

3.3.1 Haematoxylin & Eosin (H-E)

Hematoxylin and eosin stain (H&E) is referred to as the "routine stain" in histopathology, and it is used in all tissue specimens to reveal the underlying tissue structures and conditions. Hematoxylin reacts like a basic dye with a purplish blue colour. It stains acidic, or basophilic, structure including the cell nucleous (which contains DNA and nucleoprotein), and organelles that contain RNA such as ribosomes and the rough endoplasmic reticulum. Eosin is an acidic dye that is typically reddish or pink. It stains basic, or acidophilic, structures which includes the cytoplasm, cell walls, and extracellular fibres.

Harris' Hematoxylin and Eosin (H&E) Staining Protocol (8):

Reagents

- **Acid Alcohol Solution (1%)**:

Hydrochloric acid	*1 mL*
70% ethanol	*50 mL*

- For its preparation, all ingredients should be well mixed.

- **Ammonia Water Solution (0.2%)**:

Ammonium hydroxide (concentrated)	*2 mL*
Distilled water	*1000 mL*

- For its preparation, all ingredients should be well mixed.

- **Lithium Carbonate Solution (Saturated)**:

Lithium carbonate	*1,54 g*
Distilled water	*100 mL*

- For its preparation, all ingredients should be well mixed.

- **Eosin Stock Solution**:

Eosin Y	*1 g*
Distilled water	*100 mL*

- For its preparation, all ingredients should be well mixed, in order to be dissolved.

- **Phloxine Stock Solution**:

Phloxine B	*1 g*
Distilled water	*100 mL*

- For its preparation, all ingredients should be well mixed, in order to be dissolved.

- **Eosin-Phloxine B Working Solution**:

Eosin stock solution	*100 mL*
Phloxine stock solution	*10 mL*
Ethanol (95%)	*780 mL*
Glacial acetic acid	*4 mL*

- For its preparation, all ingredients should be well mixed.

- **Hematoxylin Solution (Harris)**:

Potassium or ammonium (alum)	100 g
Distilled water	1000 mL

- For its preparation, the solution was heated so as to dissolve. Then, 50 ml of 10% alcoholic hematoxylin solution was added and heated to boil for 1 minute. It was then removed from heat and slowly 2.5 g of mercuric oxide (red) were added. The solution was heated until it became dark purple color. The solution cooled in cold water bath and 20 ml of glacial acetic acid (concentrated) were added. Finally, it was filtered.

Assay

The slides were deparaffinized by immersing 2 times in xylene, 10 minutes each. Then, they were re-hydrated in 2 changes of absolute alcohol, 5 minutes each. The slides were immersed in 95% alcohol for 2 minutes and 70% alcohol for 2 minutes. Then, they were washed briefly in distilled water. The slides were stained in Harris hematoxylin solution for 8 minutes and then washed in running tap water for 5 minutes. Differentiated in 1% acid alcohol for 30 seconds and washed with running tap water for 1 minute. Bluing in 0.2% ammonia water or saturated lithium carbonate solution for 30 seconds to 1 minute and then washed in running tap water for 5 minutes. Rinsed in 95% alcohol, 10 dips and counterstained in eosin-phloxine solution for 30 seconds to 1 minute. Dehydrated through 95% alcohol, 2 changes of absolute alcohol, 5 minutes each. Finally, the slides were cleared in 2 changes of xylene, 5 minutes each and mounted with xylene based mounting medium.

3.3.2 Periodic-Acid Schiff Stain (PAS)

PAS stain is mainly used for staining red, structures containing a high proportion of carbohydrates and carbohydrate rich macromolecules such as glycogen, glycoproteins and proteoglycans. Tissues that contain these substances are connective tissues, mucus, cartilage, basement membranes, glomerular capillary basement membranes and brush borders of kidney tubules. Often used to stain kidney biopsies. It will be a useful tool

to distinguish proximal from distal convoluted tubules, as the latter do not present a brush border (Sahota et al, 2013).

Reagents

- **Periodic Acid Solution** :

Periodic Acid	*1 gram*
Distilled water	*100 mL*

- **Schiff's Reagent** :

Fuchsin Basic	*1 gram*
Distilled water	*100 mL*
Sodium metabisulphite	*2 gram*
Conc. HCl	*2 mL*
Charcoal activated	*0,3 gram*

- For its preparation, basic fuchsin was dissolved in boiling water, cooled at 50°C and filtered. Sodium metabisulphite and HCl were added. The solution was stored at dark room at room temperature overnight. Charcoal was added, shaked for one minute and filtered.

Assay

The sections were brought to distilled water and treated with periodic acid for 5 minutes. Then, they were rinsed well in distilled water and covered with Schiff's reagent for 5-15 minutes. Washed in running tap water for 5-10 minutes and counter stained with Herri's hematoxylin for approximately 15 seconds. Differentiated (if necessary) with acid alcohol and bluing as usual and washed in tap water. Finally, the

slides were rinsed in increasing concentration of alcohol (70, 80, 95 and 100%) and cleared in xylene (9).

3.3.3 Jone's Methenamine Silver (JMS)

This stain is used for demonstrating the glomerulus in kidney biopsies, as it is superior to PAS in depicting glomerular capillary basement membranes. Immune deposits, amyloid infiltration, breaks in glomerular capillary basement membranes or Bowman's capsule can be seen, as well as, tubulitis and mitotic characteristics because of the silver stain's affinity to chromatin. Vascular wall disruption can be identified, too, due to the staining of elastic lamina of arteries.

Reagents

- **1% Periodic Acid**:

Periodic acid	*5 gram*
Distilled water	*500 mL*

-For its preparation, the substances were well mixed. The solution is stable for 6 months.

- **5% Borax**:

Sodium borate	*5 gram*
Distilled water	*100 mL*

-For its preparation, the substances were well mixed. The solution is stable for 6 months.

- **Working Methenamine Solution**:

Stock methenamine silver	*50 mL*
5% borax	*6 mL*

- The solution was prepared fresh, the day of the analysis and discarded after use.

- **Stock Methenamine Silver Solution**:

3% Methenamine	*400 mL*
5% Silver nitrate	*20 mL*

-For its preparation, acid clean glassware was used. The solution was stored in the refrigerator and is stable for 6 months.

- **0.2% Gold Chloride**:

1% Gold Chloride	*1 mL*
Distilled water	*50 mL*

- For its preparation, acid clean glassware was used. The solution was stored in the refrigerator and is stable for 6 months.

- **5% Hypo**:

Sodium thiosulfate	*200 gram*
Distilled water	*4 L*

-For its preparation, sodium thiosulfate was dissolved into solution. The solution was stored in gallon jar.

- **Routine Hematoxylin and Eosin stain.**

Assay

The slides were deparaffinized and hydrated to distilled water. Then, 1% Periodic acid was added and the slides were placed in 60°C waterbath for 15 minutes. The slices were immersed 3 times in distilled water. Working methenamine solution and one coplin jar of distilled water were added and slices were placed in the microwave (high power) for 60 seconds. Then, slides were dipped in hot distilled water, silver solution was agitated and slides were added to silver solution. The coplin jar of silver solution was placed in

60°C waterbath and checked every 2- 5 minutes. The slides were allowed to remain in silver solution until sections became light brown, and a check was performed under the microscope for black membranes. The slides were rinsed in distilled water and then dipped 20 times in 0.2% Gold chloride until gray. The slides were rinsed in distilled water again. 5% Hypo was added for 1 minute to the slides and then they were washed in water. Following, counterstaining in hematoxylin for 1-3 minutes occurred, acid rinse, blue and wash in water. Finally, the slides were counterstained lightly in eosin (6, 7).

3.3.4 Masson's trichrome

This stain is helpful in evaluating the amount of collagenous connective tissue fibers in tissue specimens. Tri-chrome means that the technique produces three colours. Nuclei and other basophilic (basic-liking) structures are stained blue, cytoplasm, muscle, erythrocytes and keratin are stained bright-red and collagen is stained green or blue, depending on which variant of the technique is implemented. It is used to detect diseases or changes in these tissues.

Reagents

- **Bouin's Fixative**:

Saturated picric acid	*1500 mL*
Formaldehyde	*500 mL*
Glacial acetic acid	*100 mL*

- For its preparation, the ingredients were well mixed. The solution is stable for 2 years.

- **Biebrich Scarlet**:

Biebrich scarlet	*2,7 gram*
Acid fuchsin	*0,3 gram*

Distilled water	*300 mL*
Glacial acetic acid	*3 mL*

- For its preparation, the ingredients were well mixed. The solution is stable for 6 months

- **<u>Weigert's Iron Hematoxylin</u>**:
  - ✓ **Solution A**:

Hematoxylin	*5 gram*
95% alcohol	*500 mL*

- For its preparation, the ingredients were well mixed. The solution is stable for 1 year

  - ✓ **Solution B**:

29% ferric chloride	*20 mL*
Distilled water	*475 mL*
Hydrochloric acid	*5 mL*

- For its preparation, the ingredients were well mixed. The solution is stable for 1 year.

- **<u>Weigert's Hematoxylin</u>**:

  Working Solution: Solution A (25 ml), Solution B (25 ml)

- For its preparation, the ingredients were well mixed. The solution is stable for 3 - 4 days.

- **<u>Phosphotungstic/ Phosphomolybdic Acid Solution</u>**:

Phosphotungstic acid	*25 gram*
Phosphomolybdic acid	*25 gram*
Distilled water	*1000 mL*

- For its preparation, the ingredients were well mixed. The solution is stable for 6 months.

- **Aniline Blue**:

Aniline blue	*2,5 gra,*
Distilled water	*100 mL*
Glacial acetic acid	*1 mL*

- For its preparation, the ingredients were well mixed. The solution is stable for 6 months.

- **1% Acetic Acid**:

Glacial acetic acid	*10 mL*
Distilled water	*1000 mL*

- For its preparation, the ingredients were well mixed. The solution is stable for 1 year.

Assay

*Mordant in Bouin's solution,put in the microwave for 1 minute, allowed to stand for 15 minutes and then washed in running tap water for 5 minutes, to remove the picric acid. Weigert's working hematoxylin was added, for 10 minutes. Blue in running tap water for 5 minutes and then rinsed in distilled water. Biebrich scarlet was then added for 5 minutes. Rinsed in distilled water. Phosphotungstic/phosphomolybdic acid was added for 10 minutes, and the solution

was discarded. The slides were transferred directly into Aniline blue for 5 minutes and then rinsed in distilled water. 1% Acetic acid was added for 1 minute, the solution was discarded and the slides were rinsed in distilled water. Finally, the slides were dehydrated, cleared, and coverslipped (10).

*Conventional method: Mordant in Bouin's solution, 60°C for 1 hour.

3.4 Detection of apoptosis

There are various ways for the detection of apoptosis, depending on the molecular events correlated with apoptosis and the type of sample examined. The detection of nuclear DNA fragmentation is a widely accepted method to assess apoptosis in situ, by incorporating labeled nucleotides onto the free 3' OH ends of DNA fragments using a terminal deoxynucleotidyl transferase enzyme (TdT). This method is known as the TUNEL **(T**dT- mediated d**U**TP-biotin **n**ick **e**nd- labeling) assay and it offers the monitoring of apoptosis in tissue sections, providing the opportunity to histologically localize the apoptotic events.

TACS•XL®-DAB In Situ Apoptosis Detection Kit was used**.** This kit presents of a novel approach for the detection of apoptosis, based on the incorporation of nucleotides conjugated to bromodeoxyuridine (BrdU) at the 3’ OH ends of the DNA fragments that are created during apoptosis. This detection system uses a biotin conjugated anti-BrdU antibody, streptavidin-horseradish peroxidase and the colorimetric substrate diaminobenzidine (DAB) (Figure 5).

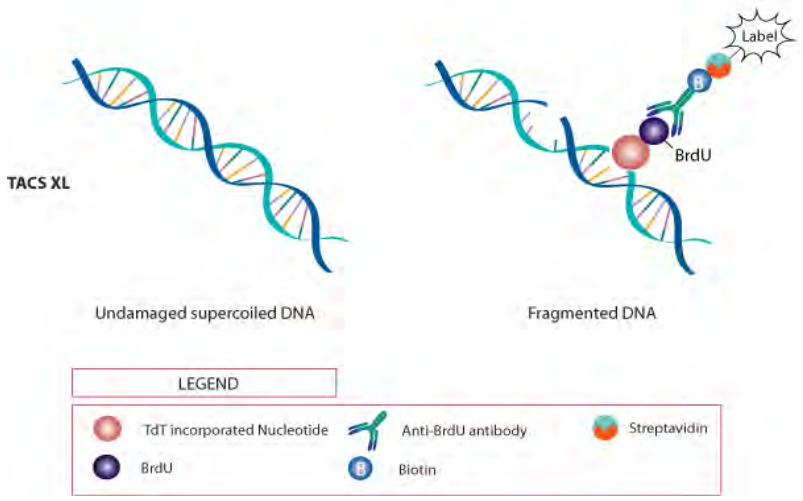

Figure 5: Simplified scheme depicting the mechanisms of TACS XL assay

Reagents

- **1 x PBS**:

- For its preparation, 10x PBS were diluted to 1x by using distilled water. 500 mL of 1x PBS were used to process up to 10 samples.

- **PBST**:

1x PBS	*200 ml*
Tween®20	*100μL*

- For its preparation, the above ingredients were mixed. 200 mL of the solution were used to process up to 10 slides.

- **3,7% Buffered Formaldehyde**:

37% formaldehyde	*5 ml*
10x PBS	*5 ml*
H_2O	*40 ml*

- For its preparation, the above ingredients were mixed. 50 mL of freshly prepared fixative were used to process up to 10 slides.

- **Proteinase K Solution**:

Deionized water	*50μL per sample*
Proteinase K	*1 μL per sample*

- For its preparation, deionized water and Proteinase K were mixed. 50 μL of Proteinase K Solution was used per sample.

- **Cytonin**:

- Cytonin is ready to use. 50 μL were used per sample.

- **Quenching Solution**:

Methanol	*45 mL*
30% hydrogen peroxide	*5 mL*

- For its preparation, the above ingredients were mixed. 50 mL were used to process up to 10 samples.

- **TdT Labelling Buffer**:

-For its preparation, the 10x TdT Labelling buffer were converted to 1x by using distilled water. 50 mL of the 1x Labelling Buffer were used to process up to 10 samples.

- **Labelling Reaction Mix**:

B- dNTP Mix	*1μL per sample*
TdT enzyme	*1 μL per sample*
1x TdT Labelling Buffer	*50 μL per sample*

- For its preparation, the above ingredients were mixed.

- **TdT Stop Buffer**:

- For its preparation, the 10x TdT Stop buffer were converted to 1x by using distilled water. 50 mL of the 1x Labelling Buffer were used to process up to 10 samples.

- **Antibody Solution**:

Anti- BrdU	*1 μL per sample*
Strep- Diluent	*50 μL per sample*

- For its preparation, the above ingredients were mixed. 50 μL of diluted antibody were used per sample.

- **Strep-HRP Solution**:

1xPBS	*50 μL per sample*
Strep-HRP	*1 μL per sample*

- For its preparation, the above ingredients were mixed. 50 μL of Strep- HRP Solution were used per sample.

- **DAB Solution**:

1x PBS	*50 mL*
DAB	*250 μL*
DAB Enhancer	*0 to 50 μL*
30% hydrogen peroxide	*50 μL*

- For its preparation, the above ingredients were mixed. 50 mL of DAB Solution were used to process up to 10 samples.

- **1% Methyl Green**:

-Methyl Green was ready to use.

- **Xylenes**:

- Xylenes were ready to use.

- **100%, 95%, 70% Ethanol**:

- 100% ethanol was diluted with deionized water to prepare 95% and 70% solutions.

- **TACS-Nuclease™ and Buffer**:

TACS-Nuclease™ Buffer	*50 μL per sample*
TACS- Nuclease	*1 μL per sample*

- For its preparation, the above ingredients were mixed.

Assay

Hydrated, fixed, and immobilized samples were immersed in 1x PBS for 10 minutes. The samples were then covered with 50 μl of Proteinase K Solution for 15-30 minutes, or with 50 μl of Cytonin^{TM} for 30 minutes, and then washed two times in deionized water (2 minutes each). The samples were immersed in Quenching Solution for 5 minutes and then washed in 1x PBS for 1 minute. The samples were immersed in 1x TdT Labeling Buffer for 5 minutes. The samples were then covered with 50 μl of Labeling Reaction Mix and were incubated for 60 minutes at 37 ^{o}C in a humidity chamber. Afterwards, samples were immersed in 1x TdT Stop Buffer for 5 minutes and washed two times in 1x PBS (2 minutes each). Samples were covered with 50 μl of Antibody Solution, and incubated for 30 minutes at 37 ^{o}C and then washed two times in 1x PBS (2 minutes each). The samples were covered with 50 μl of Strep-HRP Solution, incubated for 10 minutes at room temperature and washed two times in 1X PBS (2 minutes each). Then, the samples were immersed in DAB Solution for 2 to 7 minutes and washed in deionized water 2 times (2 minutes each). The samples were immersed in 1% Methyl Green for 30 seconds up to 5 minutes. Dipped ten times each in 2 changes of deionized water, 95%, and then 100% ethanol. Dipped, then, 10 times each in 2 changes of xylenes. Finally, glass coverslips were mounted using mounting medium.

Apoptotic cells show fragmented or condensed appearance and are painted brown with DAB. (1, 11, Ulukaya et al, 2011))

3.5 Statistical analysis

The statistical package SPSS 20.0 (Statistical Package for Social Sciences, SPSS) was used for data analysis. For the statistical analysis, *mean*, *standard deviation* and *standard error* were calculated first for each sample. Oxidative stress biomarkers were analyzed with one- way analysis of variance (ANOVA) followed by Tukey's post hoc test and Dunnet's test for multiple pairwise comparisons. Values were considered to be statistically significant at a level of $p < 0,05$. All computations were performed with SPSS, 20.0 (Statistical Package for Social Sciences Inc., Chicago, IL, USA). Values are presented as mean ± SEM.

These two test are used because they are non- parametric, as we do not know if there is normal distribution due to the small sample size. ANOVA test tells you whether you

have an overall difference between your groups, but it does not tell you which specific groups differed – post hoc tests do. Because post hoc tests are run to confirm where the differences occurred between groups, they should only be run when you have a shown an overall statistically significant difference in group means (i.e., a statistically significant one-way ANOVA result). Post hoc tests attempt to control the experimentwise error rate (usually alpha = 0.05) in the same manner that the one-way ANOVA is used instead of multiple t-tests. Post hoc tests are termed *a posteriori* tests; that is, performed after the event (the event in this case being a study)

4. Results

4.1. Renal biochemical parameters

As shown in Figure 6, urea and creatinine measurements follow the same pattern as compared to the control group: there is an increase up to the 24h measurement that is then declining until the final measurement in 48 hours.

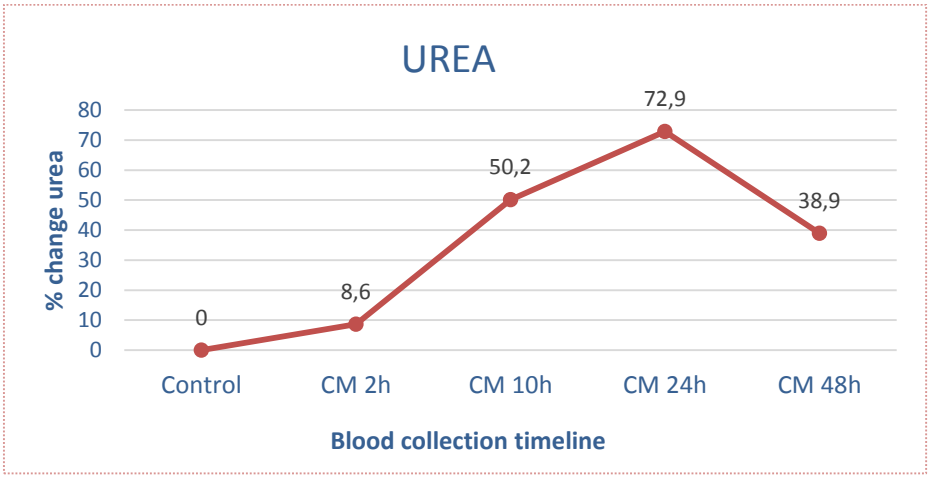

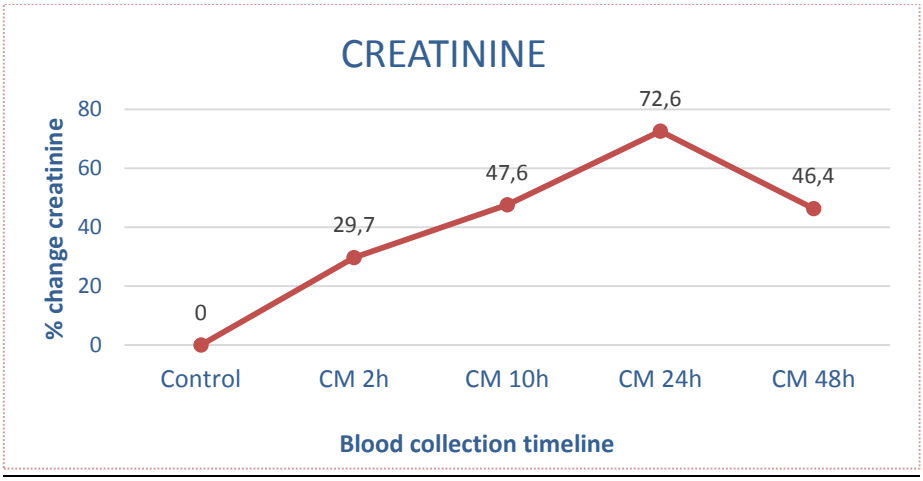

Figure 6: Mean values of biochemical parameter measurements.

4.2. Oxidative stress biomarkers

In order to assess the oxidation- reduction status of kidney tissues before and after the administration of iodinated contrast media, multiple comparisons were made between the three regional parts of the kidney in each group as well as in the same anatomic area between the control and CIN- treated groups.

4.2.1. Catalase

Catalase measurement in the cortical area of the kidney, showed a statistically significant reduction between 48hour and control groups (-39,6%) as well as between 48hCIN and 24hCIN groups (-33,3%). There was no statistically significant difference in the other areas of the kidney (juxtamedullary, medullary) between the three groups. In the juxtamedullary area, we observe a slight increase in catalase levels between 24hCIN and control group (10,9%), that decrease further in 48hCIN group (-39,6%). Finally, in the medullary area, a decline in catalase levels is observed between 24CIN and control group (-19,8%) that is further decreased in the 48hCIN group (-6,3%).

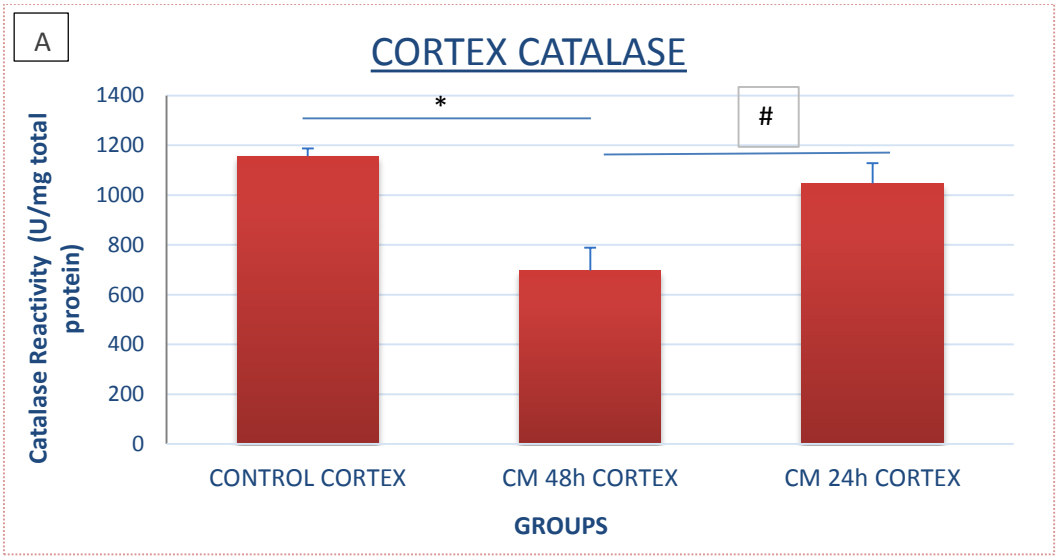

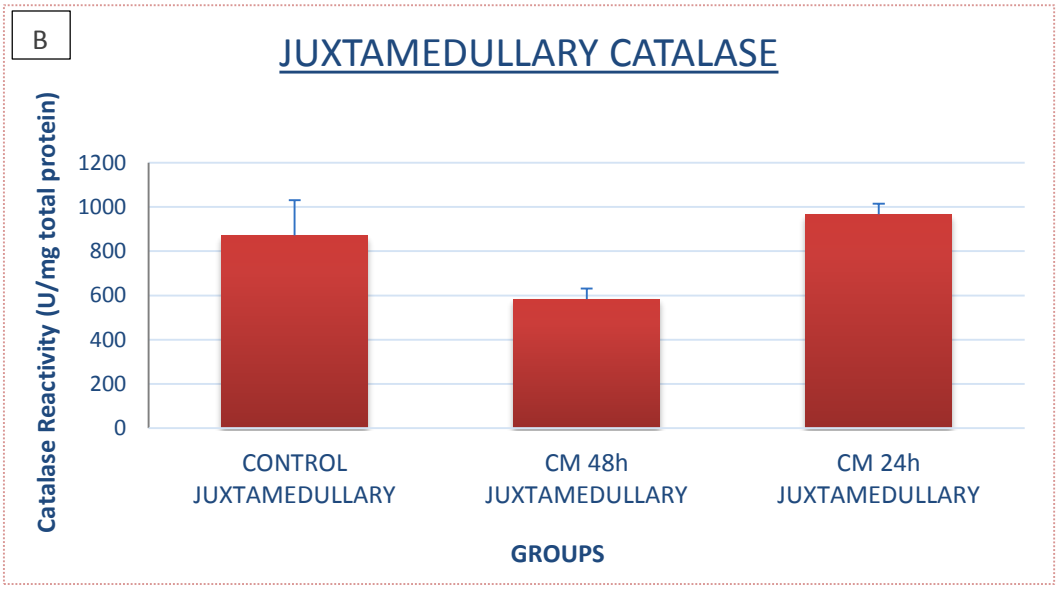

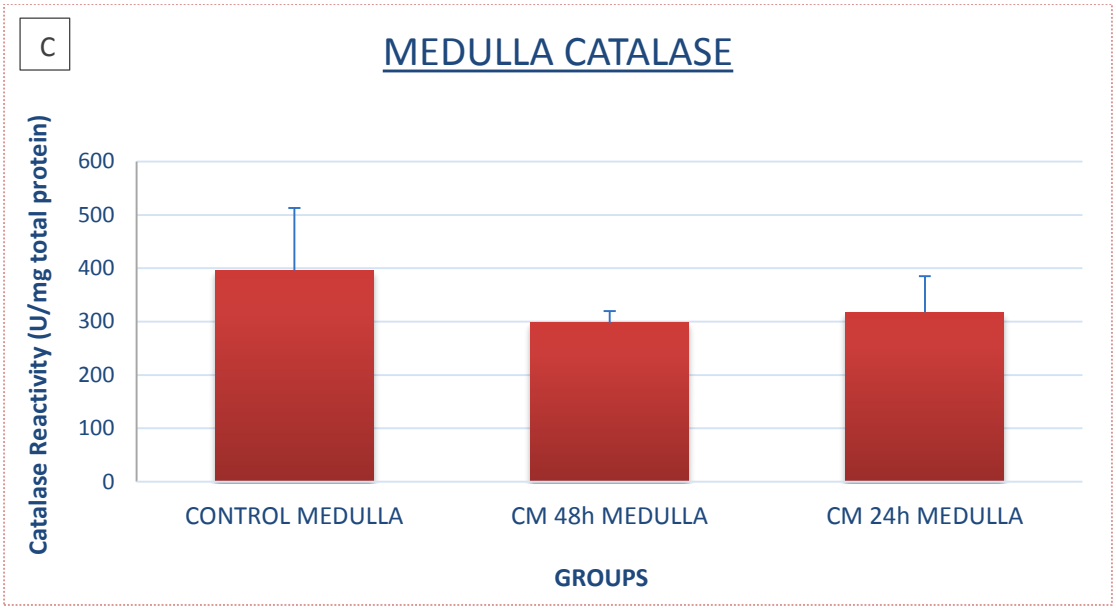

Figure 7 : Catalase levels in each region of the kidney. A significant difference was observed in A: cortical region between the groups that did not occur in B: juxtamedullary and C: medullary areas of the kidney tissue.

Furthermore, a comparison was performed between the mean values of three regional parts of the kidneys in the same group of animals. As shown in Figure 8 below, catalase levels are significantly increased in the cortical region compared to the medullary in the *Control group* (*191,9%*) and in the 24h CIN group (*229,9%*) but not in the 48h CIN group. In *24h CIN group*, catalase levels are significantly higher in juxtamedullary compared to the medullary area (*204,7%*). No statistically significant differences were observed in *48h CIN group*, where catalase levels where higher in the juxtamedullary compared to the medullary area (*96,2%*) and the cortical area showed a slight increase compared to the juxtamedullary region (*19,6%*).

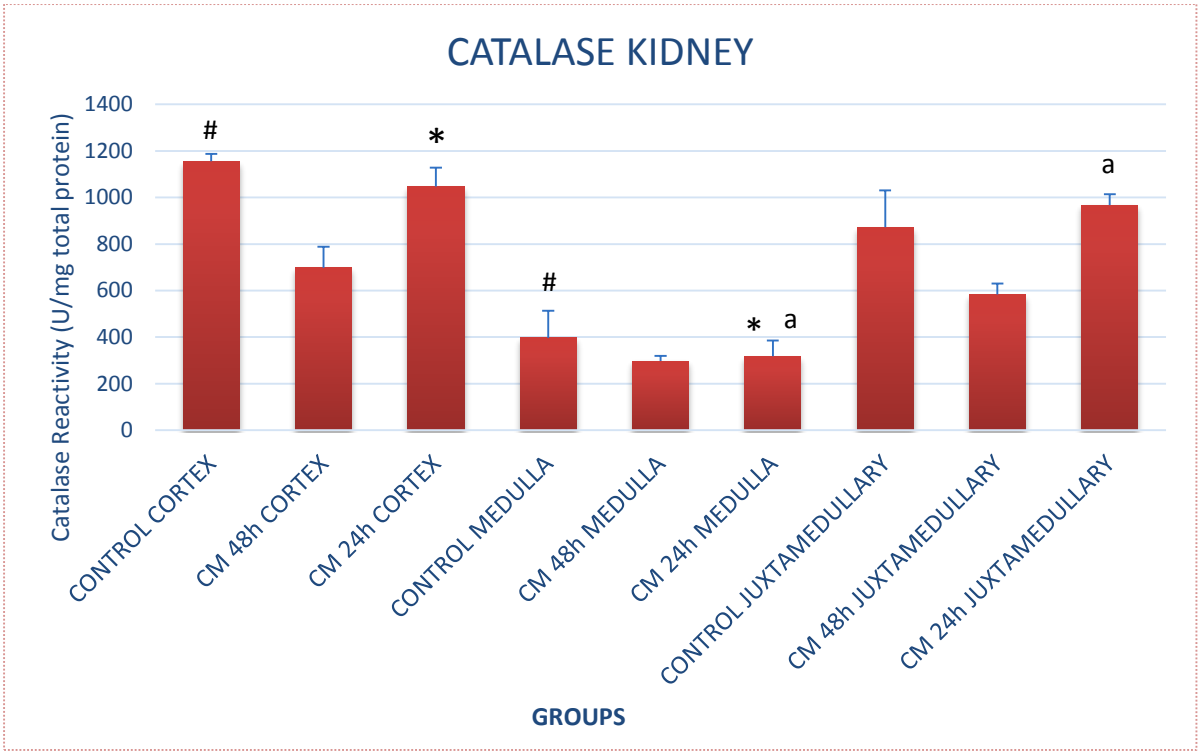

Figure 8 : Overall mean values of cortical, medullary and juxtamedullary parts of the kidneys in Control, 24 hour and 48 hour CIN groups

4.2.2. Total Antioxidant capacity (TAC)

No significant differences were noted in TAC levels in cortical, juxtamedullary and medullary areas between the control and CIN- treated groups (Figure 9). In the cortical region, TAC levels were slightly higher in 24h CIN group compared to the control group (*7,6%*) and were then decreased in 48h CIN group (*-17,7%*). The same pattern is also observed in the other regions of the kidney, too. In the juxtamedullary region, TAC levels were higher in 24h CIN group compared to the control group (6,3%) and were then decreased in 48h CIN group (-17,8%). Finally, in the medullary region, TAC levels were higher in 24h CIN group compared to the control group (*9,1%)* and were then decreased in 48h CIN group (-26,6%).

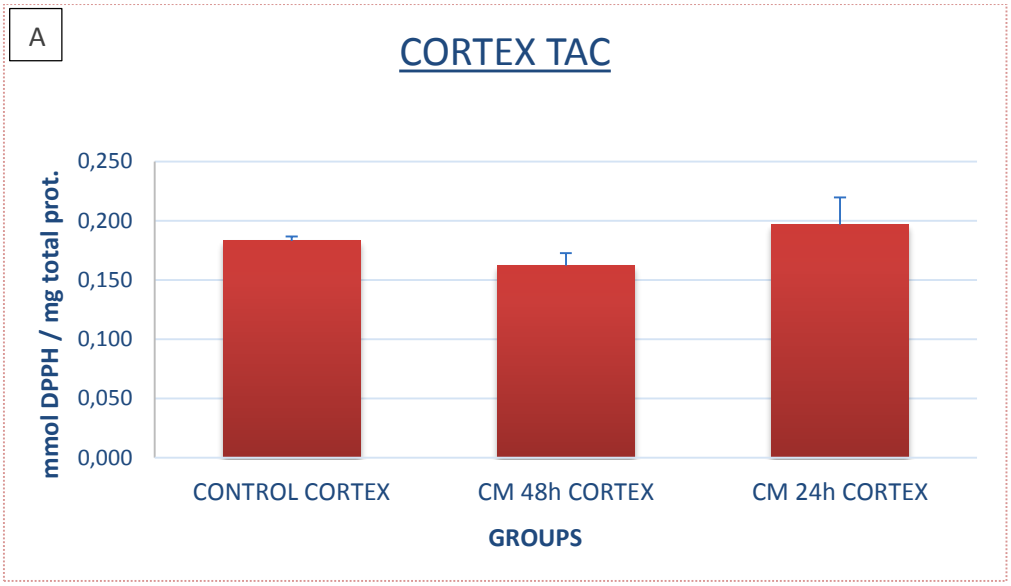

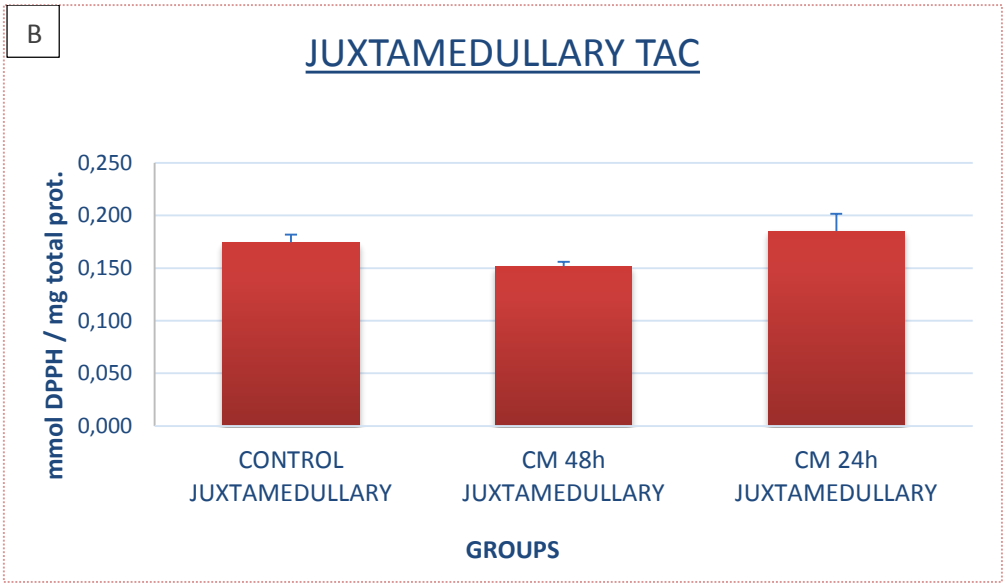

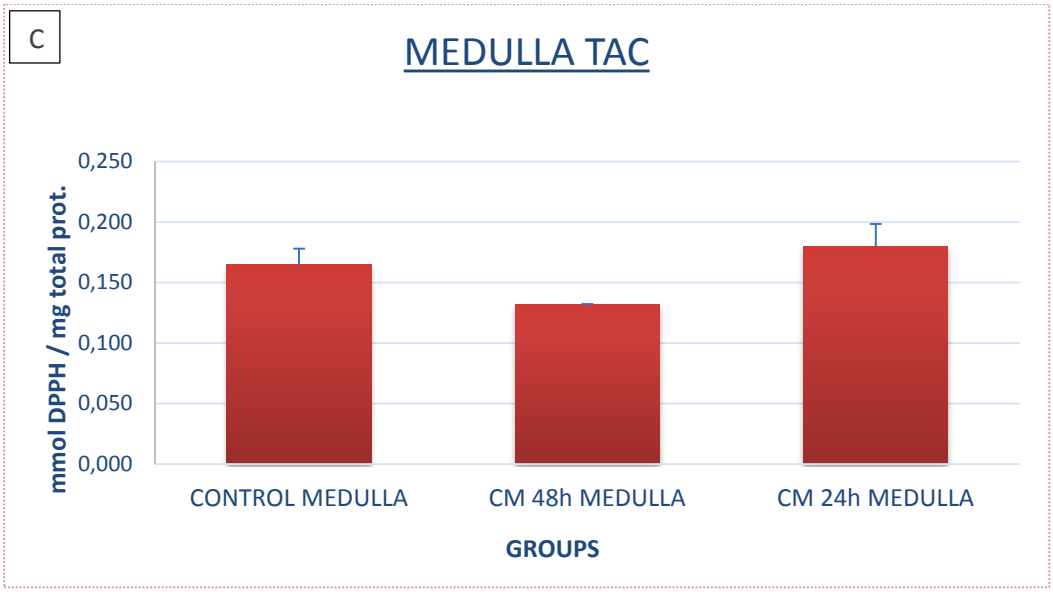

Figure 9: Mean values of TAC measurement in A: cortical region B: juxtamedullary and C: medullary region in all groups.

Furthermore, a comparison was performed between the mean values of the three regional parts of the kidneys in the same group of animals. As shown in Figure 10 below there is not any significant difference in any group. However, all groups follow the same pattern: TAC levels are lower in the medullary region, slightly higher in the juxtamedullary region and then slightly higher in the cortical compared to the juxtamedullary region. More specifically, in the *Control group*: TAC levels in juxtamedullary area were 5,4% higher than medullary and in the cortical 5,1% higher than the juxtamedullary area. In the *24h CIN group*, TAC levels in juxtamedullary area were 2,7% higher than medullary and in the cortical area 6,4% higher than the juxtamedullary area. Finally, in the *48h CIN group* TAC levels in juxtamedullary area were 15,2% higher than medullary and in the cortical 6,5% higher than the juxtamedullary area.

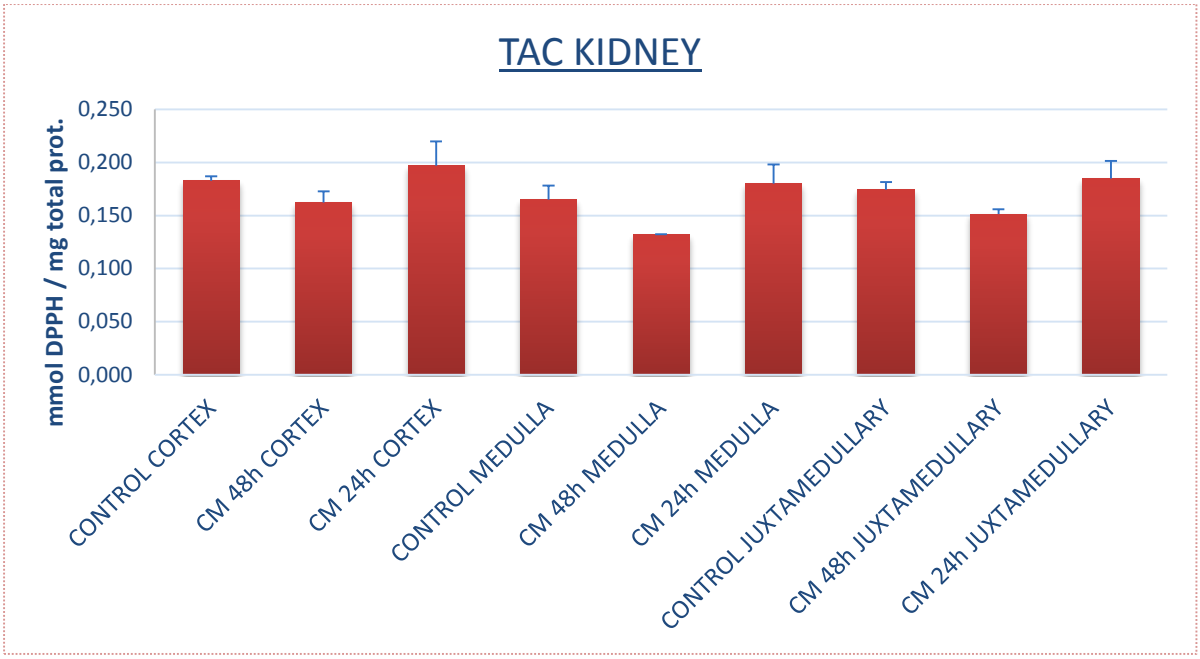

Figure 10: Overall mean values of cortical, medullary and juxtamedullary parts of the kidneys in Control, 24 hour and 48 hour CIN groups

4.2.3. Protein Carbonyls (PC)

No significant differences were noted in PC levels in cortex, juxtamedullary and medullary areas between the control and CIN- treated groups (Figure 11). TBARS levels in cortical and juxtamedullary regions follow the same pattern: control groups show the higher TBARS levels that are markedly reduced in 24h and 48h CIN groups (-62,3%, and -4,6% for cortical, -51,7% and -9,5% for juxtamedullary areas respectively). However, in the medullary area, the lower TBARS levels are observed in the control group, that are transiently increased in 24h CIN group (339,8%) and declining at the 48h CIN group (-26,9%).

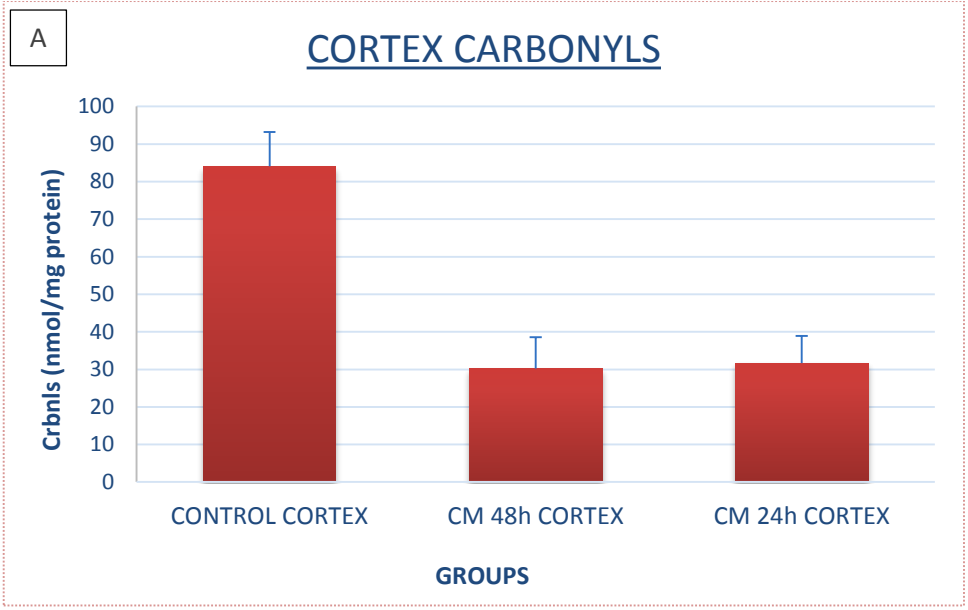

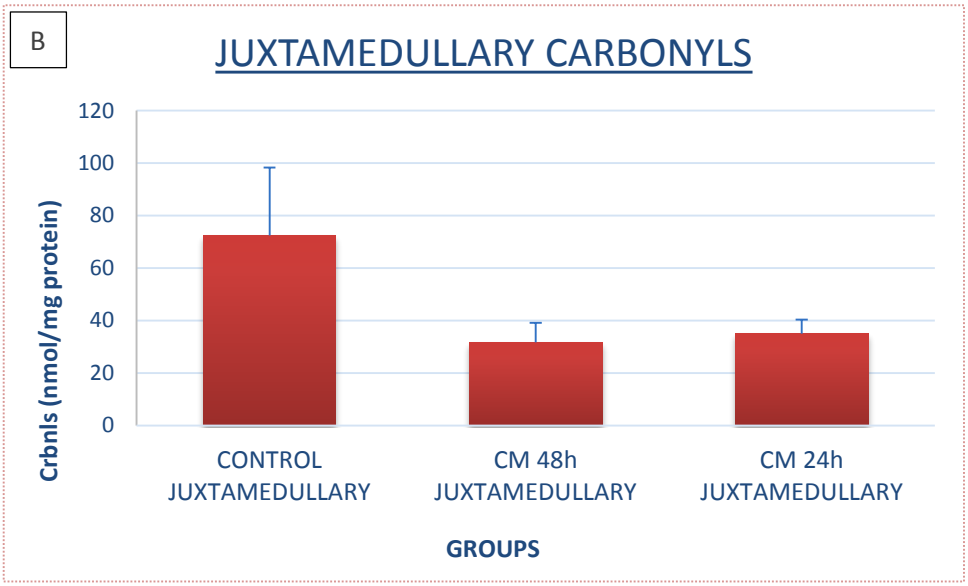

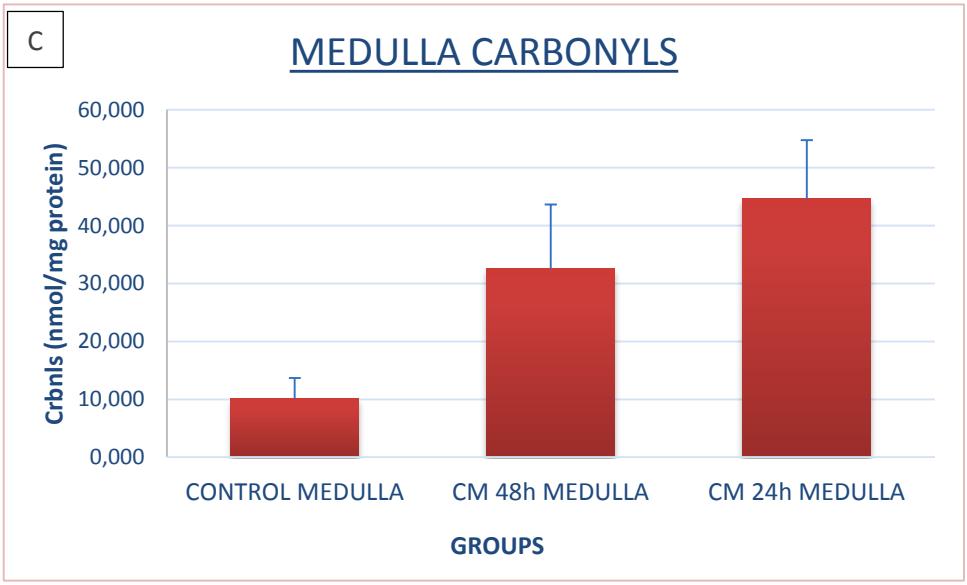

Figure 11: Mean values of PC measurement in A: cortical region in all groups, B: juxtamedullary region in all groups, C: medullary region in all groups.

Furthermore, a comparison was performed between the mean values of three regional parts of the kidneys in the same group of animals (Figure 12). In the *Control group*, the lower levels are observed in the medullary region, increasing in the juxtamedullary (*613,8%*), and the cortical (*16,1%*) region. In the *24h -CIN group* the lower levels are observed in the cortical region, increasing in the juxtamedullary (*10,4%*), and medullary region (*27,6%*). In the *48h-CIN group*, the lower levels are observed in the cortical region, increasing in the juxtamedullary (*4,8%*) and medullary (*2,8%*) areas.

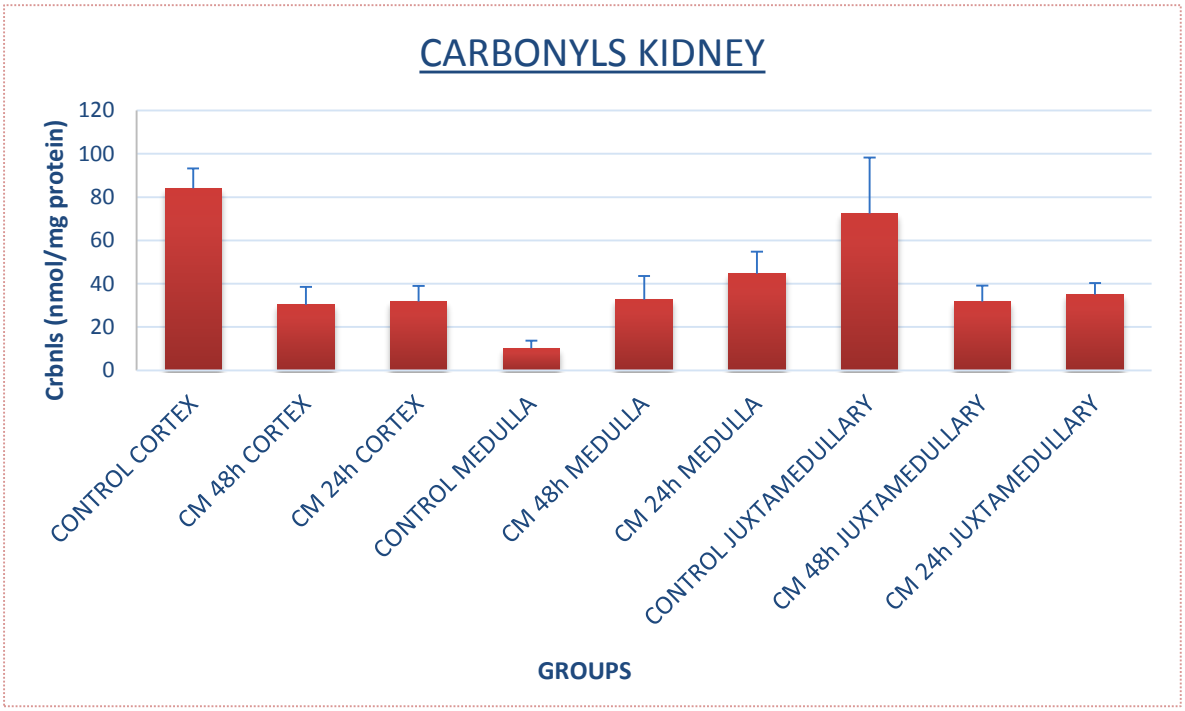

Figure 12: Overall mean values of cortical, medullary and juxtamedullary parts of the kidneys in Control, 24 hour and 48 hour CIN groups.

4.2.4. TBARS

No significant differences were noted in TBARS levels in cortical, juxtamedullary and medullary areas between the control and CIN- treated groups (Figure 13). We can observe the same pattern in cortical and medullary kidney regions. TBARS levels

decline in the 24h CIN group as compared to the control group and in the 48h CIN group. More specifically, in the cortical region, there is a reduction of *-46,6%* between 24h CIN and control group, that further decreased in the 48h CIN group (*-23,6%*) as compared to 24h CIN group. In the medullary region, there is a reduction of *-29,6%* between 24h CIN and control group that further declined in the 48h CIN group (*-20,6%*). However, in the juxtamedullary area, we observe a transient increase in TBARS level in 24h CIN group as compared to the control group (7%) that is further decreased in the 48h CIN group (*-12,9%*).

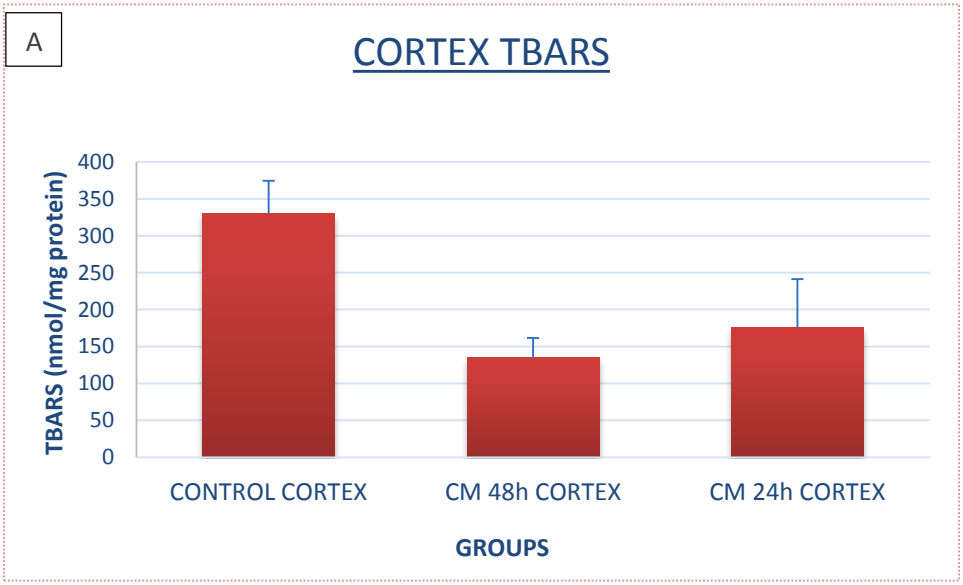

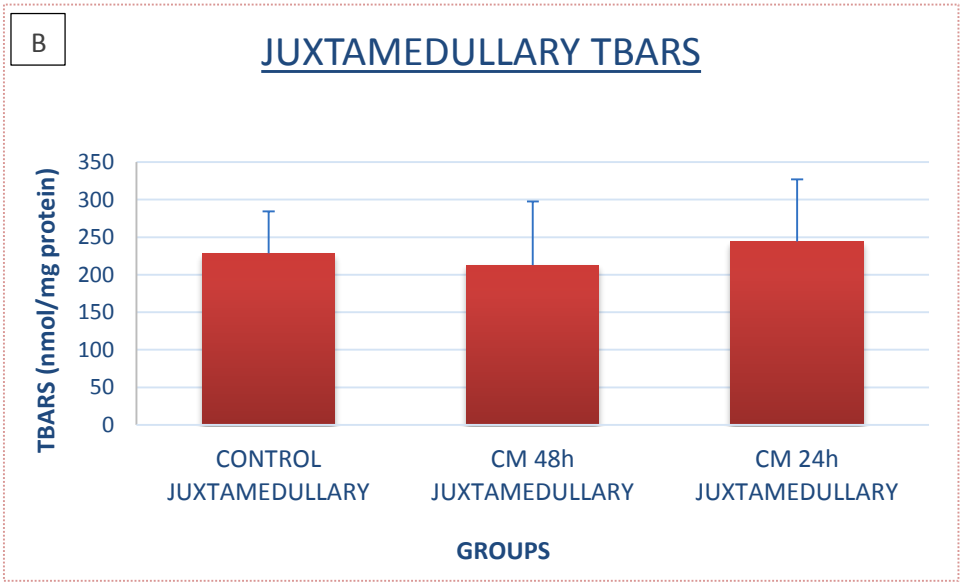

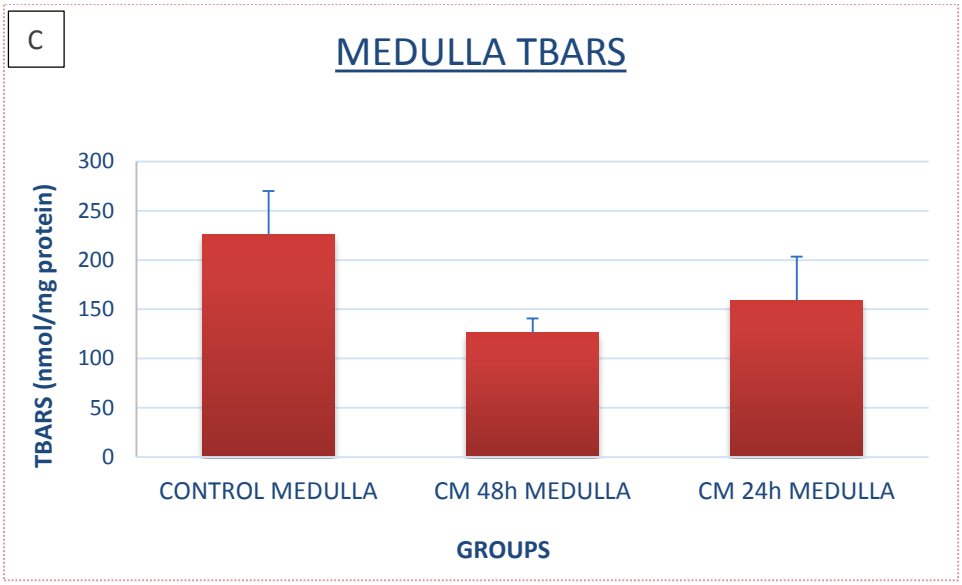

Figure 13: Mean values of TBARS measurement in A: cortical region in all groups, B: juxtamedullary region in all groups, C: medullary region in all groups.

Furthermore, a comparison was performed between the mean values of three regional parts of the kidneys in the same group of animals (Figure 14), and no statistically significant differences were observed. In the *Control group*, medullary area showed the lowest TBARS levels, that slightly increased in the juxtamedullary (*1,3%*) and cortical (*44,4%*) areas. As far as CIN treated groups are concerned, we observe another pattern: the lower TBARS levels are observed in the medullary region, increasing in the cortical and juxtamedullary regions. More specifically, in the *24h- CIN group* TBARS levels in the cortical area were 10,8% higher than the medullary and further increase (38,9%) in juxtamedullary area. Finally, in the *48h- CIN group*: cortical 6,7% higher than medullary and further increase 58,2% in juxtamedullary area

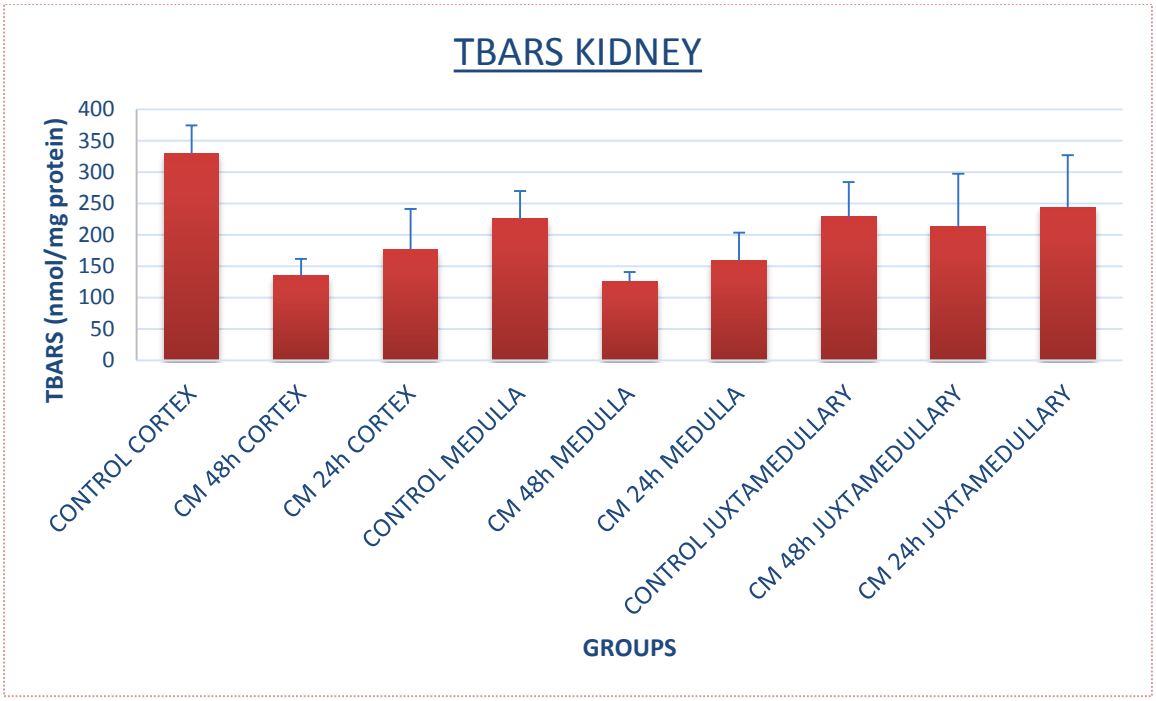

Figure 14: Overall mean values of cortical, medullary and juxtamedullary parts of the kidneys in Control, 24 hour and 48 hour CIN groups.

4.3. Histopathological evaluation

No pathological findings were noted in kidney samples from the Control group with all stains (Figure 15). In CIN- treated groups, extensive tubular vacuolization and necrosis was observed in proximal convoluted tubules (mainly observed with *H&E*) that extended to the outer stripe of the outer medulla, whereas the inner stripe is almost normal (Figures 16, 17). Proteinaceous casts in medullary tubular ducts, mostly in the inner zone of the medullary area were observed. In *PAS* stain the brush border of proximal convoluted tubules is well depicted and hyaline droplets are evident in CIN treated groups (Figure 19). *Masson's trichrome* stain did not show any stain- specific lesions (fibrosis), as the tubular damage is acute and collagenous connective tissue fibers are absent.

There were no significant differences between 24-hour and 48- hour harvested kidney tissues. Vacuolization in proximal convoluted tubules was noted in both 24-h and 48-h groups, but was more extensive in the former. 48-h group presented a higher percentage of necrotic tubules. Interstitial inflammation was also present in the cortical area. However, glomeruli were intact in both groups, assessed mainly with *Jone's*

Methenamine Silver stain that is specialized in this specific part of the nephron (Figure 16).

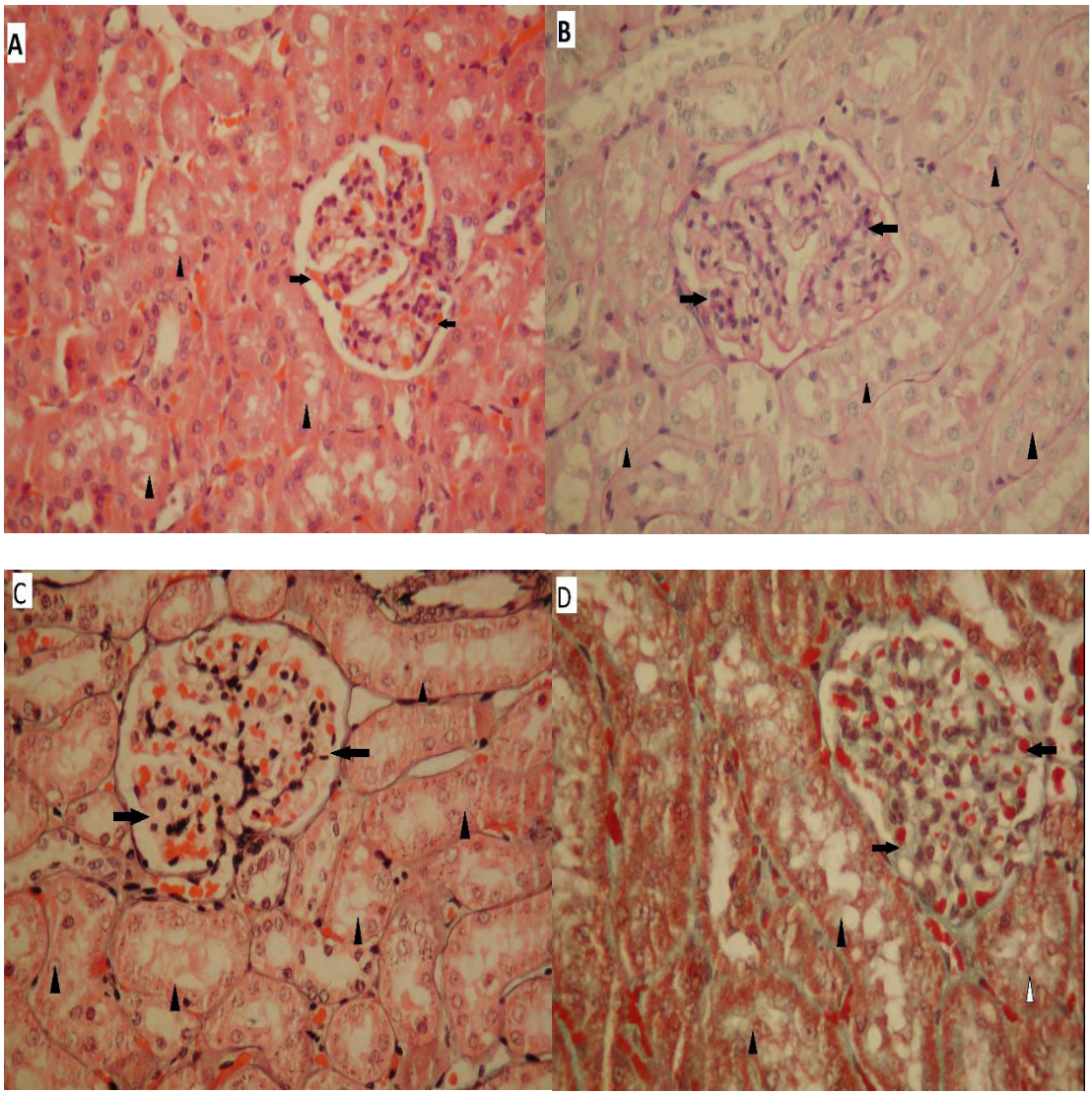

Figure 15: Representative images from Control group. Cortical region with normal glomeruli (arrow) and proximal convoluted tubules (arrow heads). *(A: H&E,* B: *PAS*, C: *Jone's Methenamine Silver*, D: *Masson's trichrome*) *(200x magnification)*

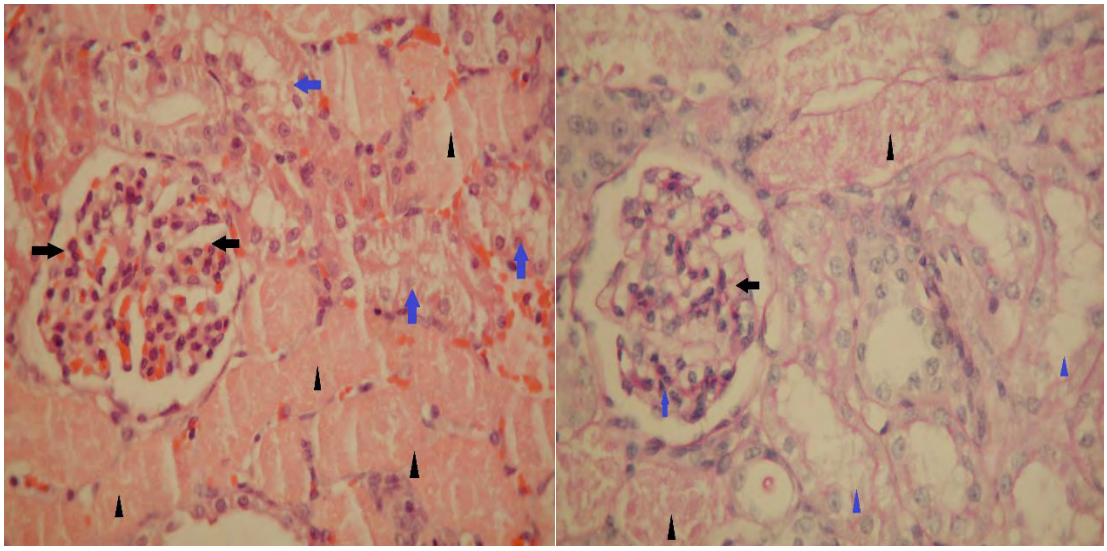

Figure 16: Renal cortex in CIN- treated kidneys. Tubular necrosis (arrow heads) and tubular vacuolization (blue arrows) are dominant, whereas glomeruli remain intact (black arrows). (Left: *H&E*, Right: *PAS*) *(200x magnification)*

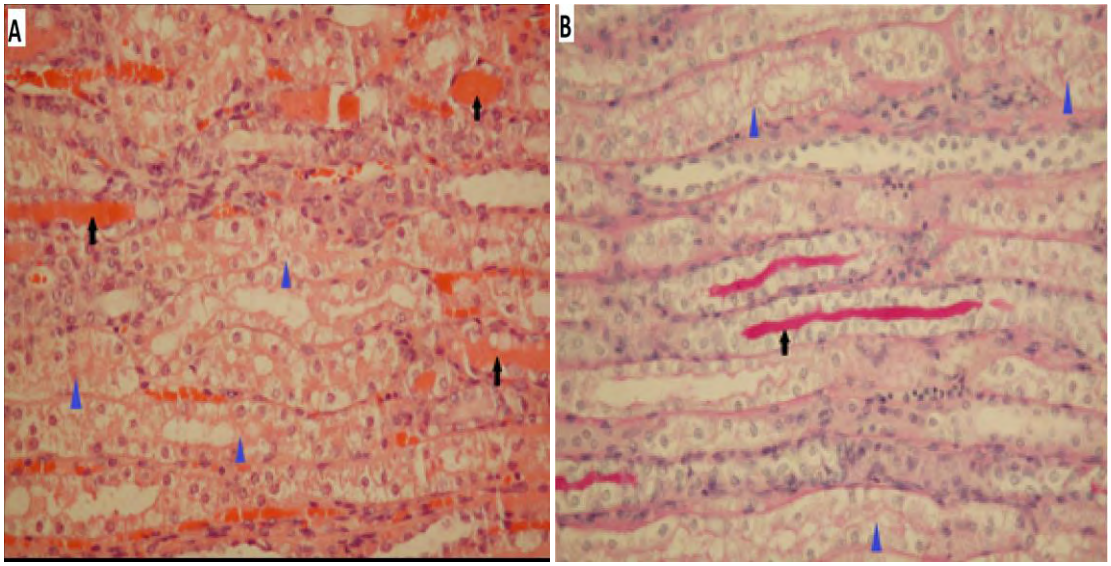

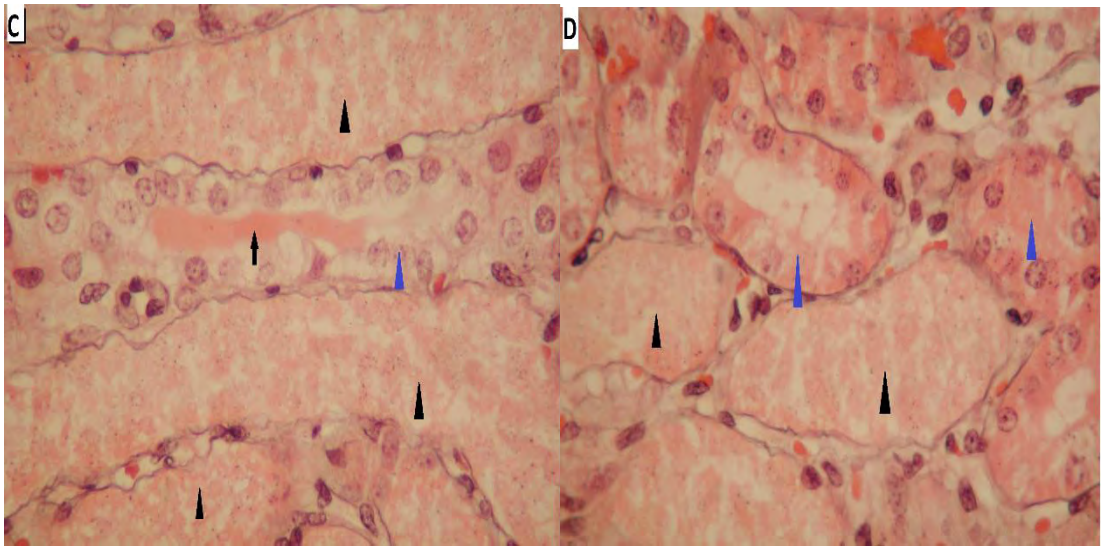

Figure 17: Outer Stripe of the outer medulla in CIN- treated kidneys. Extended tubular vacuolization (blue arrow heads) is noted, few proteinaceous casts in tubular lumen, that appear as pink homogenous material (arrows) and necrosis (black arrow heads). (A: *H&E*, B: *PAS,* C, D: *Jason's Methenamine Silver*) *(200x magnification)*

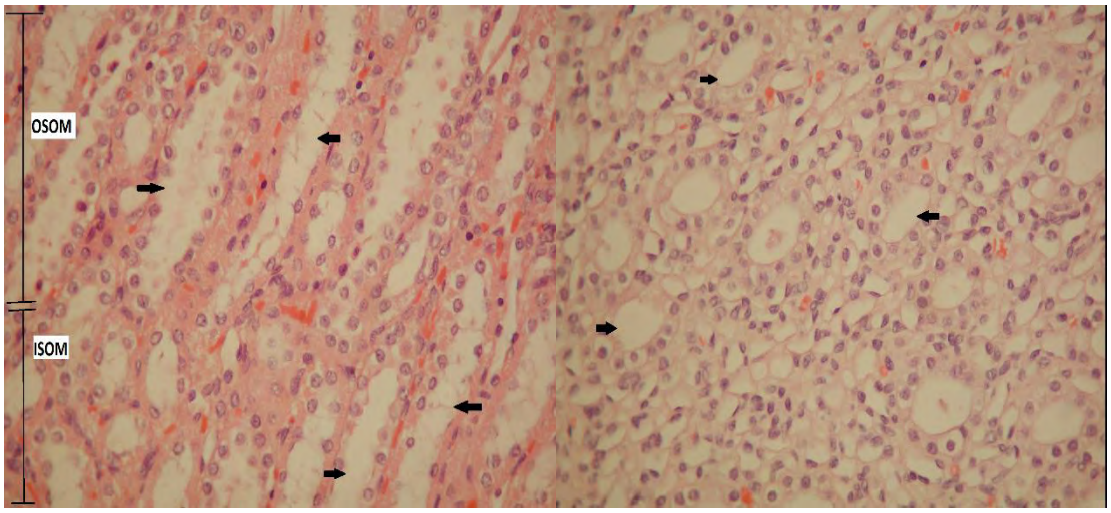

Figure 18: Outer medulla zone of CIN- treated kidneys. Left: Transitional zone from the outer stripe of the outer medulla (OSOM) to the inner stripe of the outer medulla (ISOM) where extended vacuolization is evident (arrows). Right: Inner stripe of the outer medulla where collecting tubules (arrows) are distinguished. (*H&E*) *(200x magnification)*

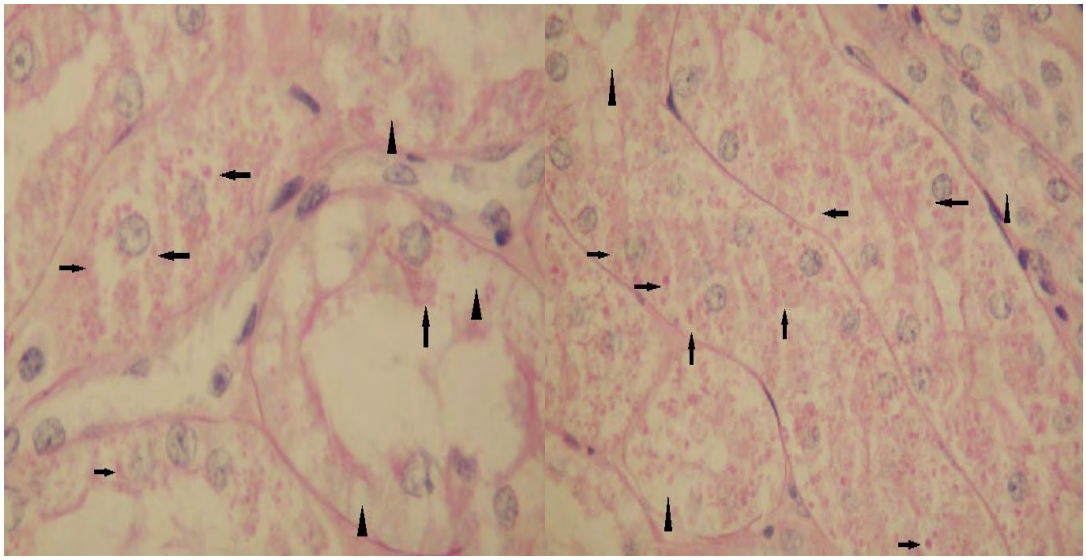

Figure 19: Outer medulla zone in CIN- treated kidneys. An abundance of hyaline droplets are shown within tubular cells (arrows) with extended vacuolization (arrow heads). (*PAS*) *(200x magnification)*

These histopathological findings were then scored (Table 3). The scoring system was the following: ***0***= *no damage*, ***1***= *mild damage* (less than 25%), ***2***=*moderate damage* (between 25 and 50%), ***3***= *severe damage* (between 50 and 75%), ***4***= *very severe damage* (more than 75%).

Control group	**Cortex**	**Juxtamedullary**	**Medulla**
Tubular necrosis	0	0	0
Vacuolization	0	0	0
Proteinaceous casts	0	0	0
24h-CIN group	**Cortex**	**Juxtamedullary**	**Medulla**
Tubular necrosis	3,25	3,25	1
Vacuolization	3,25	3,25	2,25
Proteinaceous casts	0	0	2,6
48h-CIN group	**Cortex**	**Juxtamedullary**	**Medulla**

Tubular necrosis	3,67	3,67	1
Vacuolization	3	3	2,33
Proteinaceous casts	0	0	2,25

Table 3 : Haematoxylin & Eosin scoring (mean values)

4.4. Detection of apoptosis

TUNEL staining did not show any apoptotic features in cortical, juxtamedullary or medullary regions of the kidneys in the Control as well as in CIN-treated groups, as compared to the positive control, where brown areas indicate apoptotic regions (Figure 20).

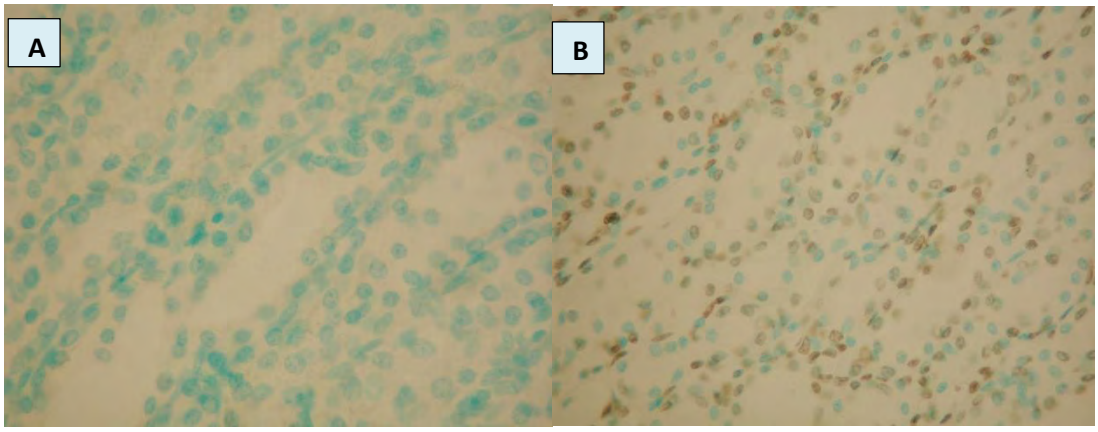

Figure 20 : A: Representative image from CIN-treated groups, outer zone of the outer medulla. No apoptosis was observed**. B: Image from the Positive control:** brown areas indicate apoptotic effects *(200x magnification)*

4.5. Kidney to body weight ratio

At baseline, there were no significant changes in mean body weight between the Control group and CIN- treated groups (Table 5) as well as in kidney to body weight ratio in all groups. As shown in Table 6, a slight increase is observed in kidney to body weight ratio in CIN- treated groups.

Animal Groups	Initial body weight	Final Body weight
Control group	3,31 kg	3,21 kg
24h CIN group	3,38 kg	3,39 kg
48h CIN group	3,55 kg	3,41 kg

Table 4 : Mean Body weight of control and CIN-treated groups before CM- administration, after 24 hours (24h CIN group) and after 48 hours (48h CIN group).

Animal Groups	Kidney/ BW ratio
Control group	2,66
24h CIN group	2,97
48h CIN group	2,8

Table 5 : Mean Kidney to Body Weight ratio of Control and CIN-treated groups

4.6. Biochemical parameters- Histopathology Correlations

A correlation was made between the histopathological scoring and biochemical parameters, using the *Chi-square (χ^2) test for association*. The statistical evaluation showed that tubular vacuolization in cortical and juxtamedullary regions was statistically correlated with serum creatinine levels (r=0.875, p=0.021) and creatinine changes through the time points (chi square 7, df=3, p=0050) as well as with the levels of serum urea (r=0.787, p=0.023). However, there was no statistical correlation between necrosis or proteinaceous casts and biochemical parameters.

5. Discussion

Contrast-induced nephropathy (CIN) is the third leading cause of hospital- acquired renal insufficiency globally, after the intravascular administration of iodinated contrast media in radiographic and interventional procedures. Its pathophysiology remains unclear and involves ischemic phenomena, ROS production and direct renal tubular toxicity. However, it is difficult to provoke CIN in animals with normal renal function, and animal models (mainly rats) are exposed to multiple renal insults involving

ischemia or nephrotoxic drugs. This gap may limit the extent to which results from laboratory animals can be extrapolated to the human situation. We attempted to shed more light to the pathophysiological mechanism, using *the rabbit nephrotoxicity model*, as described before by the research groups of *Petterson* and *Lauver* (Pettersson et al, 2002, Lauver, 2014).

As previous authors suggested, the ideal preclinical model for CIN should meet three major criteria: it should not be lethal, in order to be comparable to the clinical human condition, intravenous administration of common contrast- media should lead to a significant increase in serum urea and creatinine and standard histopathological changes should be easily seen with routine stains (Linkermann et al, 2013). This model fulfilled all these conditions with the advantage of lacking previous insults. Our rabbit nephrotoxicity model involved healthy animals with normal renal function.

To our knowledge, this is the first study in New Zealand White rabbits that examined oxidation- reduction status separately in three different areas of kidney tissues (cortical, juxtamedullary, medullary regions). We speculated that the different PO_2 in these areas may lead to different levels of ROS production. The results of these measurements were correlated with serum biochemical levels, histopathological lesions and apoptotic phenomena after intravenous administration of the non-ionic, low-osmolar, iodinated contrast- medium, *iopromide (*Ultravist®*)*.

As far as serum biochemical parameters are concerned, there was an increase in serum creatinine levels >25% in 2 hours after contrast- media administration. This showed that contrast- induced nephropathy was provoked in all animals. As shown in Figure 6, urea and creatinine mean levels were rising until 24 hours after administration and then begun to decline until our final measurement at 48 hours. These findings lead to the assumption that after 10- 24 hours there was a counterbalance from the rabbit's defense mechanisms. *Lauver and colleagues* showed that creatinine begun to rise in 1-2 hours and peaked at 48 hours after cm- administration (Lauver et al, 2014).

Histopathological evaluation showed extended vacuolization in proximal convoluted tubules of the cortical region, as well as in the outer zone of the medullary area in CIN-treated animals (Figure 16). *Tubular vacuolization* is a degenerative change associated with a variety of toxic substances. Contrast- agents are taken up within tubular cells by

pinocytosis and pinocytic vessels fuse with lysosomes forming larger vacuoles (Dickermann et al, 2008).Vacuolization induced by xenobiotics is characterized by clear to translucent spaces of different shapes inside a pale or granular cytoplasm. Usually cells are swollen and nuclei is displaced. Vacuole formation may come as an early stage of necrosis or accompany specific types of tubular injury, such as intracellular accumulation of fluid, glycogen or lipids (Sahota et al, 2013). It is an early sign of CIN and without co-existing factors it might not progress to necrosis (Dickermann et al, 2008). This condition is also described as "osmotic nephrosis" as it is provoked after the intravascular administration of osmotically active compounds, such as contrast- media (Sahota et al, 2013). However, this term is misleading (Randhawa et al, 1999) because the reason of the swelling in tubular epithelial cells is not osmotic pressure but the formation of vacuoles (Dickermann et al, 2008). As far as *proteinaceous casts* are concerned, they represent a fluid accumulation or cell breakdown products that fill the tubular lamina. They may be the result of increased permeability of the glomerulus that results in tubular proteinosis (Sahota et al, 2013). They usually appear in distal segments and collecting ducts (Greaves, 2012). Literature refers to vacuolization (Shih-Ping et al, 2010, Ozkan et al, 2012) and proteinaceous casts (Ari et al, 2012, Liu et al, 2014, Ozkan et al, 2012) mainly in rat models.

The most important histopathological lesion related to contrast- media acute nephrotoxicity is *necrosis,* especially in proximal convoluted tubules. Acute test- article related injury is associated with various stages of tubular degeneration that may result in localized (single cells affected) or generalized (the whole epithelium is affected) necrotic phenomena (Sahota et al, 2013). Previous research has shown a prevalence of necrotic phenomena in CIN- treated groups in rat (Buyuklu et al, 2015, Ozkan et al, 2012, Ari et al, 2012) and rabbit (Lauver et al, 2014) experiments. Our results confirm this theory as generalized necrosis is present in CIN –treated groups (Figures 16, 17). Proximal convoluted tubules are more prone to necrosis following xenobiotic administration than medullary collecting ducts or distal convoluted tubules. Proximal tubular epithelium is the region of the kidney where the most of the membrane-bound active transport activity occurs. It has increased permeability to ions and chemical influx than distal tubular epithelium, due to the higher electrical resistance and tighter intracellular junctions found in the latter (Sahota et al, 2013).

As mentioned above, vacuolization in cortical and juxtamedullary areas was statistically correlated with serum creatinine levels and fluctuations as well as with serum urea levels. This phenomenon did not occur neither with the other histopathological lesions nor in the medullary area. This finding is of utmost importance, as it is shown that biochemical parameters that are easily and non-invasively measured in the blood can provide valuable information about the situation of renal tubules.

When chronic injury occurs, there may be a disruption of the basement membrane that could result in tubular atrophy and interstitial fibrosis (Sahota et al, 2013). Masson's Trichrome stain did not depict any signs of fibrous connective tissue as, in our study the animals were euthanized in 24-48 hours in the acute phase of nephrotoxicity.

Catalase levels in cortical region were significantly higher in 24hour than 48hour CIN groups and between Control and 48hour groups (Figure 7). A rapid decline in catalase levels is observed after the first 24 hours that follow contrast- media administration, but only in the cortical region. Medullary and juxtamedullary areas do not show significant differences. This consumption of catalase in CIN- treated groups probably shows that the enzyme was "used" due to oxidative damage in the cortical area, which was more prominent in 48 hour harvested tissues than in 24hour ones. These results are in accordance to the histopathological lesions of the kidneys, as tubular necrosis and vacuolization are prominent in the cortical region of the kidney tissues in these groups.

Vasoconstriction, ROS production and direct tubular cellular toxicity are three interconnected mechanisms, as mentioned above. As far as literature is concerned, in vivo studies that used animal models susceptible to CIN have demonstrated prolonged vasoconstriction of the renal vasculature, especially in the cortical and outer medullary regions of the kidney (Heyman et al 1991, Nygren, 1992) in accordance with our histopathological findings. *Colbay and colleagues*, also showed that catalase is consumed in CIN- treated rat kidneys and they attributed it to oxidative damage (Colbay et al, 2010). On the other hand, *Garofalo and colleagues* performed an in vitro experimental study, using proximal porcine renal tubules (LLC-PK1) and Mardin-Darby canine kidney distal tubular renal cells (MDCK) and they failed to demonstrate a correlation between contrast- media administration and ROS production, as MDA levels, hydrogen peroxide and superoxide anion were not increased and antioxidant

agents did not protect the cells. Necrosis and apoptosis were present (Garofalo et al, 2007). *Zager and colleagues* studied the possible pathways of CIN in vitro, in proximal tubular renal cells derived from mice and humans. Contrast-media administration did not augment MDA levels and the antioxidant agents such as SOD, catalase, glutathione and oxypurinol failed to present protective effects against renal tubular injury. They even tried to reversely approach oxidative stress by blocking endogenous antioxidant pathways but this did not mediated insults either. All these results lead to the conclusion that oxidative stress could not be associated with CIN- induced damage (Zager et al, 2003).

In contrast to our results, there is plenty of research data indicating increased MDA levels in CIN- treated groups, which are, as mentioned above, end- products of lipid peroxidation of membrane polyunsaturated fatty acids by free radicals and indicators of oxidative damage (Ari et al, 2012, Buyuklu et al, 2015, Liu et al, 2014, Ozkan et al, 2012).

As far as apoptosis is concerned, TUNEL method failed to confirm any related activity in kidney tissues that were harvested at 24 (24h CIN group) and 48 (48h CIN group) hours after iodinated contrast- media administration. There are two theories that could explain this result:

On the one hand, we could suggest that cell death is not associated with apoptosis, based on TUNEL and histopathological evaluation (no characteristic apoptotic phenomena were observed (membrane blebbing, DNA fragmentation etc). However, this should be confirmed with another method for qualitatively or quantitatively measure apoptosis, such as morphological imaging, biochemical, immunological or molecular biology techniques. The confirmation of apoptosis is recommended with at least two methods that belong in different categories, as there are overlapping characteristics between different types of cell death (Ulukaya et al, 2011). On the other hand, and taking into consideration urea and creatinine measurements, we could suggest that our results are falsely negative and apoptotic phenomena occurred before 24 hours. *Lee and colleagues* in a rat experiment showed that apoptosis in kidney tubular cells may come as early as 24 hours and precede the significant rise of serum creatinine (Lee et al, 2011). Another experiment could be performed to euthanize animals in less than 24

hours and study the possible existence of apoptotic phenomena with the proper methods.

6. Conclusion

As a conclusion, the *rabbit nephrotoxicity model* was successful, based on our biochemical and histopathological findings, and contrast- induced nephropathy occurred in animals with normal kidney function, without any prior intervention. This is very important for a correct extrapolation of the results to the human condition. Urea and creatinine levels were counterbalanced after 24 hours, when oxidative status markers showed the higher ROS production. Oxidative stress seemed to be one of the mechanisms implicated in CIN and statistical insignificance in the majority of biomarkers may be due to the low number of animals. There were no apoptotic phenomena in kidney tissues.

Future research is recommended in this rabbit model so as to cover other aspects of the condition, such as molecules implicated in the pathophysiology in order to develop relative preventive strategies. Future research may use more animals and euthanize some groups before and after our timeline, in order to have a wider view of the fluctuations of the parameters. The apoptotic pathway could be studied more thoroughly, based on our observations. Finally, one proposal would be the study of necroptosis implicated in contrast-induced nephropathy, because in vitro research data are promising and there is minimum study in vivo, related to the necroptotic pathways.

7. REFERENCES

- Aebi H, ***Catalase in vitro***, Methods Enzymol, 1984, 105:121-6
- Ari E, Kedrah E A, Alahdab Y, Bulut G, Eren Z, Baytekin O, Odabasi D, ***Antioxidant and renoprotective effects of paricalcitol on experimental contrast- induced nephropathy model,*** The British Journal of Radiology, 2012, 85: 1038- 1043
- Asif A, Epstein M. ***Prevention of radiocontrast- induced nephropathy***. American Journal of Kidney Disease, 2004, 44:12-24
- Bakris GL, Burnett GC Jr, ***A role for calcium in radiocontrast-induced reductions in renal hemodynamics***, *Kidney Int* 1985, 27:465– 468
- Barreto R. ***Prevention of contrast-induced nephropathy: the rational use of sodium bicarbonate***. Nephrol Nurs Journal, 2007, 34(4):417-421
- Bhargava AS, Hofmeister R, Siegmund F, Schobel C, Gunzel P. ***Effect of three non- ionic contrast media on rats and rabbits with regard to renal changes: interspecies comparison***. Arzneimittelforschung 1990, 40:822-829
- Bradford M. M., ***A Rapid and Sensitive Method for the Quantitation of Microgram Quantities of Protein Utilizing the Principle of Protein-Dye Binding***, Analytical Biochemistry, 1976, 72:248-254
- Brezis M, Rosen S, ***Hypoxia of the renal medulla—its implications for disease***. N Engl J Med, 1995 332:647–655
- Buyuklu M., Kandemir FM, Ozkaraca M., Set T, Bakirci EM, Topal E, Ileriturk M, Turkmen K, ***Beneficial effects of lycopene against contrast medium-induced oxidative stress, inflammation, autophagy, and apoptosis in rat kidney***, Hyman and Experimental Toxicology, 2015, 34(5):487-496
- Caiazza A., Russo L., Sabbatini M., Russo D., ***Hemodynamic and Tubular Changes Induced by Contrast Media***, BioMed Research International, 2014, article ID: 578974
- Choudhury D, ***Acute kidney injury: current perspectives***, Postgrad Med, 2010, 122 (6):29-40
- Colbay M, Yuksel S, Uslan I, Acarturk G, Karaman O, Bas O, Mollaoglu H, Yagmurca M, Ozen O A, ***Novel approach for the prevention of contrast nephropathy,*** Experimental and Toxicologic Pathology, 2010, 62: 81-89

- De Almeida S L, Barboza R J, Santos Freitas P F, Porto L M, Vasquez C E, Meyrelles S S, Gava L A, Costa Pereira M T, ***Sildenafil prevents renal dysfunction in contrast media- induced nephropathy in Wistar rats***, Human and Experimental Toxicology, 2016 1-9
- Degterev A, Huang Z, Boyce M, Li Y, Jagtap P, Mizushima N, Cuny D G, Michison J T, Moskowitc A M, Yuan J, ***Chemical inhibitor of nonapoptotic cell death with therapeutic potential for ischemic brain injury,*** Nature Chemical Biology, 2005, 1: 112-119
- Detrenis S., Meschi M., Musini S., Savazzi G., ***Lights and shadows on the pathogenesis of contrast- induced nephropathy: state of the art***, Nephrol. Dial. Transplant, 2005, 20:1542-1550
- Devrim E., Cetin M., Namuslu M., Erguder IB., Cetin R., Durak I., ***Oxidant stress due to non-ionic low osmolar contrast medium in rat kidney***, Indian J Med Res, 2009, 130:433-436
- Dickenmann M., Oettl T., Mihatsch J. M., "***Osmotic nephrosis: acute kidney injury with accumulation of proximal tubular lysosomes due to administration of exogenous solutes***," *American Journal of Kidney Diseases*, vol. 51, no. 3, pp. 491–503, 2008.
- Evola S., Lunetta M., Macaione F., Fonte G., Milana G., Corrado E., Bonura F., Novo G., Hoffmann E., Novo S. ***Risk factors for contrast induced nephropathy: A study among Italian patients***, Indian heart journal, 2012, 64: 484-491
- Fiaccadori E., Maggiore U., Rotelli C.et al., ***Plasma andurinary free 3-nitrotyrosine following cardiac angiography procedures with non-ionic radiocontrast media***, Nephrology Dialysis Transplantation, 2004, vol. 19, no. 4, pp. 865–869
- Garofalo S., Borges F.T., Dalboni M.A., Santos O. F. P. D., ***Reactive oxygen species independent cytotoxicity induced by radiocontrast agents in tubular cells (LLC-PK1 and MDCK)***, Renal Failure, 2007,vol. 29, no. 2, pp. 121–131,
- Geenen R., Kingma H., Van der Molen A., ***Contrast-induced nephropathy: pharmacology, pathophysiology and prevention,*** Insights Imaging, 2013, 4:811–820

- Golman K, Almen T, ***Uroraphic contrast media and methods of investigative radiology. In: Sovac M, ed. Radiocontrast agents***. Berlin, Germany : Springer-Verlag, 1984, 127:191
- Graur D., Duret L, Gouy M. ***Phylogenetic position of the order Lagomorpha (rabbits, hares and allies)***. Nature, 1996, 379:333
- Gruberg L, Mehran R, Dangas G, et al. ***Acute renal failure requiring dialysis after coronary interventions***. Catheter Cardiovasc Interv. 2001, 52:417-419.
- Guastoni C., Bellotti N., Poletti F et al, "***Continuous venovenous hemofiltration after coronary procedures for the prevention of contrast-induced acute kidney injury in patients with severe chronic renal failure***, The American Journal of Cardiology, 113(4):588-592, 2014
- Haschek M. W., Rousseaux G. C., Wallig A. M., ***Handbook of Toxicologic Pathology***, 3rd Edition, Academic Press, 2013, 1667-1679
- Heinrich MC, Kuhlmann MK, Grgic A, Heckmann M, Kramann B, ***Cytotoxic effects of ionic high- osmolar, nonionic monomeric, and nonionic iso-osmolar dimeric iodinated contrast media on renal tubular cells in vitro***, Radiology, 2005, 235: 843-849
- Heyman SN, Brezis M, Epstein FH, Spokes K, Silva P et al, ***Early renal medullary hypoxic injury from radiocontrast and indomethacin***, Kidney Int, 191, 40: 632- 642
- Heyman SN, Reichman J, Brezis M, ***Pathophysioloy of radiocontrast nephropathy***. Invest Radiol, 1999 34:685–691
- Heyman SN, Rosen S, Khamaisi M, Idee JM, Rosenberger C, ***Reactive oxygen species and the pathogenesis of radiocontrast nephropathy***. Invest Radiol, 2010, 45:188–195
- Heyman SN, Rosen S, Rosenberger C, ***Renal parenchymal hypoxia, hypoxia adaptation and the pathogenesis of radiocontrast nephropathy***. Clin J Am Soc Nephrol,2008 3:288–296
- Hsu P.S., Tsai J.T., Chien T.C., ***Ioxitalamate Induces Renal Tubular Apoptosis via Activation of Renal Efferent Nerve- Mediated Adrenergic Signaling, Renin Activity, and Reactive Oxygen Species Production in Rats***, Toxicological Sciences, 2010, 114 (1): 149-158

- Huang T.Y., Chen Y.Y., Lai H.Y., Cheng C.C., Lin C.T., Su S.Y., Liu H.C., Lai C.P., ***Resveratrol alleviated the cytotoxicity induced by the radiocontrast agent, ioxitalamate, by reducing the production of reactive oxygen species in HK-2 human renal proximal tubule epithelial cells in vitro***, International Journal of Molecular Medicine, 2016 37: 83-91
- Igney FH, Krammer PH**. *Death and anti-death: tumour resistance to apoptosis***. Nat Rev Cancer 2002, 2:277–88.
- Janaszewska A, Bartosz G, ***Assay of total antioxidant capacity: comparison of four methods as applied to human blood plasma***, Scan J. Clin. Lab. Invest, 2002, 62(3):231-6.
- Kane GC, Doyle BJ, Lerman A, BarsnessGW, Best PJ, Rihal CS. ***Ultra-low contrast volumes reduce rates of contrast-induced nephropathy in patients with chronic kidney disease undergoing coronary angiography***. J Am Coll Cardiol. 2008, 51:89-90.
- Katzberg RW, ***Contrast medium-induced nephrotoxicity; Which pathway?*** Radiology, 2005, 235:752–755
- Keles, M.S., Taysi, S., Sen, N., Aksoy, H., Akçay, F., ***Effect of corticosteroid therapy on serum and CSF malondialdehyde and antioxidant proteins in multiple sclerosis***. Can. J. Neurol. Sci., 2001, 28 (2), 141-143.
- Kiss N, Hamar P, ***Histopathological Evaluation of Contrast- Induced Acute Kidney Injury Rodent Models, Biomed Research International***, 2006, Article ID 3763250
- Kooiman J, Le Haen PA, Gezgin G, DeVries JPP, BoersmaD, Brulez HF et al, ***Contrast-induced acute kidney injury and clinical outcomes after intra-arterial and intravenous contrast administration: risk comparison adjusted for patient characteristics by design***. Am Heart J,2013, 165:793–799
- Kowalczyk J, Lenarczyk R, Kowalski O, et al. ***Risk stratification according to the type of impaired renal function in patients with acute myocardial infarction treated with percutaneous coronary intervention***. Kardiol Pol 2007, 65:635-643.
- Lameire N, Adam A, Becker CR, Davidson C, Mc Cullough PA, ***Baseline renal function screening***, Am J Cardiol, 2006, 98:21-26

- Lauver D. Adam, Carey E. Grant, Bergin L. Ingrid, Lucchesi R. Benedict, Gurm S. Hitinder, ***Sildenafil Citrate for Prophylaxis of Nephropathy in an Animal Model of Contrast- Induced Acute Kidney Injury***, Plos ONE, 9(11), 1-15
- Lee H. C., Chang G. J., Yen H.W., Liu H.I., Lai T.W., Sheu H.S., ***Ionic contrast media induced more apoptosis in diabetic kidney than nonionic contrast media***, JNephrol, 2011, 24(03):376-380
- Lenhard DC, Frisk AL, Lengsfeld P, Pietsch H, Jost G, ***The effect of iodinated contrast agent properties on renal kinetics and oxygenation***. Invest Radiol, 2013, 48:175–182
- Liang X, Chen Y, Zhang L, Jiang F, Wang W, Ye Z, Liu S, Yu C and Shi W: ***Necroptosis, a novel form of caspase-independent cell death, contributes to renal epithelial cell damage in an ATP-depleted renal ischemia model***. Mol Med Rep, 2014, 10: 719-724
- Linkermann A, Chen G, Dong G, Kunzendorf U, Krautwald S, Dong Z. ***Regulated cell death in AKI***, J Am Soc Nephrol 2014, 25: 2689–2701.
- Linkermann A, De Zen F, Weinberg J, Kunzendorf U and Krautwald S: ***Programmed necrosis in acute kidney injury,*** Nephrol Dial Transplant, 2012, 27: 3412-3419
- Linkermann A, Green DR. ***Necroptosis***. N Engl J Med 2014, 370: 455–465.
- Linkermann A, Heller JO, Prókai A, Weinberg JM, De Zen F, Himmerkus N, Szabó AJ, Bräsen JH, Kunzendorf U and Krautwald S: ***The RIP1-kinase inhibitor necrostatin-1 prevents osmotic nephrosis and contrast-induced AKI in mice***. J Am Soc Nephrol 24: 1545-1557, 2013.
- Liss P, Nygren A, Erikson U, Ulfendahl HR, ***Injection of low and iso-osmolar contrast medium decreases oxygen tension in the renal medulla***, Kidney Int, 1998, 53:698-702
- Liu T-q., Luo W-I., Tan Xiao., Fang Y., Chen J., Zhang H., Yu X-f., Cai J-r., Ding X-q., ***A Novel Contrast- Induced Acute Kidney Injury Model Based on the 5/6- Nephrectomy Rat and Nephrotoxicological Evaluation of Iohexol and Iodixanol In ViVo***, Oxidative Medicine and Cellular Longevity, 2014, 1-14
- Majumdar SR, Kjellstrand CM, Tymchak WJ, Hervas-Malo M, Taylor DA, Teo KK. ***Forced euvolemic dieresis with mannitol and furosemide for prevention of contrast-induced nephropathy in patients with CKD undergoing coronary***

angiography: a randomized controlled trial. *Am J Kidney Dis.* 2009, 54(4):602-609.

- Martin-Mateo M. C., Sanchez-Portugal M., Iglesias S., DePaula A., and Bustamante J., ***Oxidative stress in chronic renal failure***, *Renal Failure*, vol. 21, no. 2, pp. 155–167, 1999.
- Martinvalet D, Zhu P, Lieberman J**. *Granzyme A induces caspase- independent mitochondrial damage, a required first step for apoptosis***. Immunity 2005, 22:355–70
- McCullough PA, ***Contrast- induced acute kidney injury***, J. Am. Coll. Cardiol., 2008, 51(15):1419-1428
- Mc Cullough PA, Adam A, Becker CR, Davidson C, Lameire N et al, ***Epidemiology and prognostic implications of contrast- induced nephropathy***, Am J. Cardiol, 2006, 98:5- 13
- Moos S., van Vemde D., Stoker J., Bipat S., ***Contrast-induced nephropathy in patients undergoing intravenous (IV) contrast enhanced computed tomography (CECT) and the relationship with risk factors: A meta- analysis***, European Journal of Radiology, 2013, 82:387-399
- Norbury CJ, Hickson ID. ***Cellular responses to DNA damage***. Annu Rev Pharmacol Toxicol 2001, 41:367–401.
- Nunag M, Brogan M, Garrick R, ***Mitigating contrast- induced acute kidney injury associated with cardiac catheterization***, Cardiol. Rev, 2009, 17 (6):263-269
- Nygren A, ***Contrast media and regional renal blood flow. A study of the effects of ionic and non- ionic monomeric and dimeric contrast media in the rat***, Acta Radiol Suppl, 1992, 378 (Pt 3): 123-135
- Okamura D. M., Pennathur S., Pasichnyk K et al., ***CD36 regulatesoxidative stress and inflammation in hypercholesterolemic CKD***, Journal of the American Society of Nephrology, 2009, vol. 20, no.3, p. 495–505
- Ozkan G., Ulusoy S, Orem A, Ersoz S, Alkanat M, Yucesan B Z, Kaynar K, Al S, ***Protective Effect of the Grape Seed Proanthocyanidin Extract in a Rat Model of Contrast-Induced Nephropathy,*** Kidney Blood Press Res, 2012, 35:445–453

- Patsoukis, N., Zervoudakis, G., Panagopoulos, N.T., Georgiou, C.D., Angelatou, F., Matsokis, N.A., ***Thiol redox state (TRS) and oxidative stress in the mouse hippocampus after pentylenetetrazol-induced epileptic seizure***. Neurosci. Lett., 2004, 357, 83e86
- Patti G, Nusca A, Chello M, et al. ***Usefulness of statin pretreatment to prevent contrast-induced nephropaty and to improve long-term outcome in patients undergoing percutaneous coronary intervention***. Am J Cardiol. 2008, 101:279-285.
- Persson PB, Hansell P, Liss P, ***Pathophysiology of contrast medium-induced nephropathy***, Int Soc Nephrol, 2005, 68:14-22
- Petterson G., Toward R., Grant D., Thyberg K., Golman K., ***The Rabbit Renal Toxicity Test: A Sensitive in Vivo Test for the Nephrotoxicity of Contrast Agents***, Acad Radiol, 2002, 9:S62-S64
- Pisani A, Riccio E, Andreucci M, Faga T, Ashour M, Di Nuzzi A, Mancini A, Sabbatini M, ***Role of Reactive Oxygen Species in Pathogenesis of Radiocontrast- Induced Nephropathy***, BioMed Research International, 2013, p1-6
- Quintavalle C., Brenca M., De Micco F. et al., ***In vivo and in vitro assessment of pathways involved in contrast media induced renal cells apoptosis***, *Cell Death and Disease*, 2011, vol. 2, no. 5, article e155
- Randhawa S. P., Saad S. R., Jordan M., Scantlebury V., Vivas C., Shapiro R., ***"Clinical significance of renal biopsies showing concurrent acute rejection and tacrolimus-associated tubular vacuolization***," *Transplantation*, 1999,vol. 67, no. 1, pp. 85–89.
- Remy W. F. Geenen, Hylke Jan Kingma, Aart J. van der Molen, ***Contrast-induced nephropathy: pharmacology, pathophysiology and prevention, Insights Imaging***, 2013, 4: 811- 820
- Ribeiro L, de Assuncao e Silva F, Kurihara RS, Schor N, Mieko E, Higa S. ***Evaluation of the nitric oxide production in rat renal artery smooth muscle cells culture exposed to radiocontrast agents***. *Kidney Int* 2004;65:589 –596.
- Rizzo M, Corrado E, Coppola G, Muratori I, Novo G, Novo S. ***Markers of inflammation are strong predictors of subclinical and clinical atherosclerosis in women with hypertension***. Coron Artery Dis. 2009, 20:15-20.

- Romano G., Briguori C., Quintavaille C., Zanca C., Rivera N., Colombo A., Condorelli G., ***Contrast agents and renal cell apoptosis***, European Heart Journal, 2008, 29:2569-2576
- Rosovsky MA, Rusinek H, Berenstein A, Basak S, Setton A, Nelson PK. ***High-dose administration of nonionic contrast media: a retrospective review.*** Radiology. 1996, 200:119-122.
- Saelens X, Festjens N, Vande Walle L, van Gurp M, van Loo G, Vandenabeele P. ***Toxic proteins released from mitochondria in cell death***. Oncogene 2004, 23:2861–74
- Sahota S. P., Popp A. J., Hardisty F. J., Gopinath C., ***Toxicologic Pathology, Non Clinical Safety Assessment***, CRC Press, Florida, 2013, p 422-426
- Seeliger E., Sendeski M., Rihal S., Persson P. B., Contrast- induced kidney injury: mechanisms, risk factors, and prevention, European Heart Journal, 2012, 33(16):2007-2015
- Sendeski MM. ***The pathophysiology of renal tissue damage by iodinated contrast media.*** Clin Exp Pharmacol Physiol, 2011, 38:292–299.
- Sherwood I, ***Human Physiology: From cells to systems***, 4th ed Pacific Grove, CA Brooks/Cole, 2001:484-525
- Slee EA, Adrain C, Martin SJ. ***Executioner caspase-3, -6, and -7 perform distinct, non-redundant roles during the demolition phase of apoptosis***. J Biol Chem 2001;276:7320–6.
- Solomon R, ***Preventing contrast- induced nephropathy: problems, challenges and future directions***, BMC Med, 2009, 7:24
- Speck U, ***Contrast media: overview, use and pharmaceutical aspects***, 4th edn. Springer, Berlin Heidelberg New York, 1999, 8–83
- Stacul F, Van der Molen A, Reimer P, Webb JAW, Thomsen HS, Morcos SK, ***Contrast induced nephropathy: updated ESUR contrast media safety committee guidelines***. Eur Radiol, 2011, 21: 2527–2541
- Sterling KA, Tehrani T, Rudnick MR***. Clinical significance and preventive strategies for contrast-induced nephropathy.*** Curr Opin Nephrol Hypertens. 2008, 17:616-623.
- Stolker M.J., McCullough A.P., Rao S., Inzucchi E.S., Spertus A.J., Maddox M.T., Masoudi A.F., Xiao L., Kosiborod M., ***Pre-Procedural Glucose Levels***

and the Risk for Contrast-Induced Acute Kidney Injury in Patients Undergoing Coronary Angiography, Journal of the American College of Cardiology, 2010, vol 55, no 14, 1433-1440

- Subramanian S, Tumlin J, Bapat B, Zyczynski T. ***Economic burden of contrast-induced nephropathy: implications for prevention strategies***. J Media Econ 2007, 10(2):119–134.
- Suckow A. Mark, Schroeder Valerie, ***The Laboratory Rabbit***, 2nd Edition, CRC Press, 2010, p 5
- Thomsen HS, Morcos SK, Barrett BJ, ***Contrast-induced nephropathy: The wheel has turned 360 degrees***. Acta Radiol, 2008 49:646– 657
- Thomsen S.H., Webb A. J., ***Contrast Media Safety Issues and ESUR Guidelines***, Springer, 3rd edition, 2014
- Thomson VS, Narayanan K, Singh C***. Contrast induced nephropathy in urology***. *Indian J Urol.* 2009, 25(4):437-445.
- Tumlin J, Stacul F, Adam A, Becker CR, Davidson C, ***Pathophysiology of contrast induced nephropathy***, Am J Cardiology, 2006, 98:14-20
- Ulukaya E., Acilan C., Ari F., Ikitimur E., Yilmaz Y., ***A Glance at the methods for detection of apoptosis qualitatively and quantitatively***,Turk J. Biochem., 2011, 36(3):261-269
- Walker H. Kenneth, Hall W. Dallas, Hurst J. Willis, ***Clinical Methods, 3rd Edition, The History, Physical and Laboratory Examinations***, Butterworths, 1990
- Wang D., Chen Y., Chabrashvilli T., Aslam S., Borrego Conde L. J., Umans J. G., Wilcox C. S., ***Role of oxidative stress in endothelial dysfunction and enhanced responses to angiotensin II of afferent arterioles from rabbits infused with angiotensin II***, J. A. Soc. Nephrol., 2003, 14:2783-2789
- Wasaki M., Sugimoto J., Shirota K., ***Glucose alters the susceptibility of mesangial cells to contrast media***. Invest. Radiol. 2001, 36:355-362
- Xinway J, Xianghua F, Jing Z, et al. ***Comparison of uselfulness of simvastatin 20 mg versus 80 mg in preventing contrast induced nephropaty in patients with acute coronary syndrome undergoing percutaneous coronary intervention***. Am J Cardiol. 2009, 104:519-524.

- Zager A. R., Johnson C.M. A., Hanson Y. S., ***Radiographic contrast media-induced tubular injury: Evaluation of oxidant stress and plasma membrane integrity***, Kidney International, 2003, vol 63:p 128-139
- Zaytseva NV, Shamkhalova MS, Shestakova MV et al. ***Contrast- induced nephropathy in patients with type 2 diabetes during coronary angiography: risk factors and prognostic value***. Diabetes Res Clin Pract. 2009, 86:63-69
- Zhao Y., Tao Z., Xu Z., Tao Z., Chen B., Wang L., Li C., Chen L., Jia Q., Jia E., Zhu T., Yang Z., ***Toxic effects of a high dose of non-ionic iodinated contrast media on renal glomerular and aortic endothelial cells in aged rats in vivo***, Toxicology Letters, 2011, 202: 253-260
- Zhang Y, Wang J, Yang X, Wang X, Zhang J, ***The serial effect of iodinated contrast media on renal hemodynamics and oxygenation as evaluated by ASL and BOLD MRI***, Contrast Media Mol Imaging, 2012, 7: 418-425
- Zhang YD, Wang J, Zhang J, Wang X, Jiang X, ***Effect of iodinated contrast media on renal function evaluated with dynamic three- dimensional MR renography***, Radiology, 2014, 270: 409-415

1. https://www.rndsystems.com/resources/technical/tunel-assay-principle
2. http://www.leicabiosystems.com/pathologyleaders/an-introduction-to-routine-and-special-staining/
3. http://histology.leeds.ac.uk/what-is-histology/histological_stains.php
4. http://www.esur.org/guidelines/
5. http://www.dako.com/28829_2010_conn14_special_stains_kidney_biopsy_interpretation_laurino.pdf
6. http://library.med.utah.edu/WebPath/HISTHTML/MANUALS/JONES.PDF
7. http://library.med.utah.edu/WebPath/HISTHTML/MANUALS/HYPO.PDF
8. http://www.protocolsonline.com/histology/dyes-and-stains/haematoxylin-eosin-he-staining/
9. http://laboratoryinfo.com/periodic-acid-schiff-pas-staining-technique-for-carbohydrates/
10. http://library.med.utah.edu/WebPath/HISTHTML/MANUALS/MASSONS.PDF
11. https://www.trevigen.com/docs/protocol_4828-30-DK.pdf